P-N JUNCTION MICROWAVE PHASE MODULATORS

by

Manuel S. Navarro Stevenson

Ingeniero de Ejecucion en Electronica
Universidad Catolica de Valparaiso-Chile
(1967)

SUBMITTED IN PARTIAL FULFILLMENT OF

THE REQUIREMENTS FOR THE DEGREE OF

MASTER OF SCIENCE

at the

MASSACHUSETTS INSTITUTE OF TECHNOLOGY

August 1972

Signature of Author
Department of Electrical Engineering, August 18, 1972

Certified by
Thesis Supervisor

Accepted by
Chairman, Departmental Committee on Graduate Students

P-N JUNCTION MICROWAVE PHASE MODULATORS

by

Manuel S. Navarro Stevenson

Submitted to the Department of Electrical Engineering on August 18, 1972 in partial fulfillment of the requirements for the degree of Master of Science.

ABSTRACT

Modulator imbedding networks for semiconductor diodes are discussed. It is shown that the two-state reflection-type phase modulator, two-port imbedded is the basic circuit unit for n-state reflection or transmission-type phase modulator synthesis.

A general solution is given for reflection-type and transmission-type modulators for angles of modulation between 0 and 180^{0}. It is shown that the minimum-phase modulation angle for a given diode at a fixed frequency is determined by the implementation employed. A quantity relating Kurokawa and Schlosser's figure of merit [Proc. IEEE 58, 180-181 (1970)] and the phase difference between ON and OFF is introduced, which permits an easy calculation of losses and also the solution of the imbedding network. Broadbanding techniques are discussed and it is shown that a frequency range exists in which the "equivalent matching impedance" of the diode is resistive, which leads to a straightforward design of the matching network. It is also shown, that this particular frequency range can be determined from the theoretical model of the diode.

Thesis Supervisor: Donald H. Steinbrecher

Title: Assistant Professor of Electrical Engineering

ACKNOWLEDGEMENT

Many thanks are due to Prof. D. H. Steinbrecher for his guidance and for supervising this thesis. I also want to express my gratitude to Prof. R. L. Kyhl for helpful discussions. The collaboration of Reinaldo Spinella in preparing the microstrip circuits is greatly appreciated.

TABLE OF CONTENTS

I. INTRODUCTION

Variable-parameter devices have been used in two-state modulators for many years and the theory and limitations of RF switching and phase shifting are well known.[1-4] Considerable effort has been devoted to searching for a figure of merit for a variable-parameter one-port for RF switching or modulation,[5-7] but a general solution has not been found for lossless-reciprocal imbedding networks for phase modulators. To analyze impedance transformations through lossless reciprocal networks we shall choose an approach through non-Euclidean geometry,[8,9] where in a transformation through a lossless reciprocal network constitutes a rigid displacement. We shall use the Poncaire model, in which the absolute curve (infinite) is the unit circle, and straight lines are arc of circles cutting the absolute curve orthogonally. As usual, in standard works on non-Euclidean geometry,[10] quantities in this system will be termed "hyperbolic."

The Smith Chart Γ-plane is also the hyperbolic plane in hyperbolic geometry. No attempt will be made to obtain graphical solutions for which Deschamps'[8] Projective Chart might be used. Emphasis will be placed, however, on graphical interpretations as in any discussion concerned with geometrical models.

In this report Kurokawa and Schlosser's[5] figure of merit will be adopted, because of its analytical simplicity and peculiar characteristics.

II. REFLECTION-TYPE PHASE MODULATOR

DEFINITION. A **reflec**tion-type phase modulator is a network characterized by

$$a = \Gamma_n b, \tag{1}$$

where a and b are the incoming and outgoing signals, and Γ_n is a complex number that has n "quantized states." A physical realization of (1) has not yet been determined, and our purpose is to show that a two-state reflector-type modulator, two-port imbedded, is the basic "circuit unit" for building up an n-state reflection or transmission phase modulator.

DEFINITION. The network that performs (1) is designated NS-RM-MPI, which stands for n-state reflection modulator m-ports imbedded. The relation between m and n and the number of diodes is evident. A 2S-RM-2PI network requires one diode and a 4S-RM-3PI requires two; therefore, a general reflection-type modulator can also be identified as 2^k-RM-(k+1)PI, where k is the number of diodes. It is important to emphasize that 2^k states is the fundamental limit than can be reached, and we shall direct our discussion primarily to configurations that permit

achievement of this fundamental limit.

2.1 GENERAL CONSTRAINT IN A REFLECTION-TYPE PHASE MODULATOR

In phase modulation, amplitude modulation must be avoided. This introduces the general constraint

$$|\Gamma_1| = |\Gamma_2| = |\Gamma_3| = \ldots = |\Gamma_n|. \qquad (2)$$

Equations 2 and 1 indicate that for a constant input amplitude, the output (reflected wave) will be of the same amplitude regardless of the state. A great deal of this report is a study of the physical realizations of (2).

2.2 TWO-STATE, REFLECTION-TYPE MODULATOR, TWO-PORT IMBEDDED

The 2S-RM-2PI network, the simplest possible configuration, is shown in Fig. I. When the modulation signal is applied to the microwave diode the impedance is switched between ON and OFF, thereby causing a large mismatch and reflecting most of the incident RF energy. The impedances z_1 and z_2 (forward and reverse biased diode impedances) at RP-1 do not produce equal-amplitude reflection coefficients; therefore, a lossless-reciprocal two-port imbedding network is needed to transform these impedances to z_1' and z_2' at RP-2 (Figs. 1 and 2).

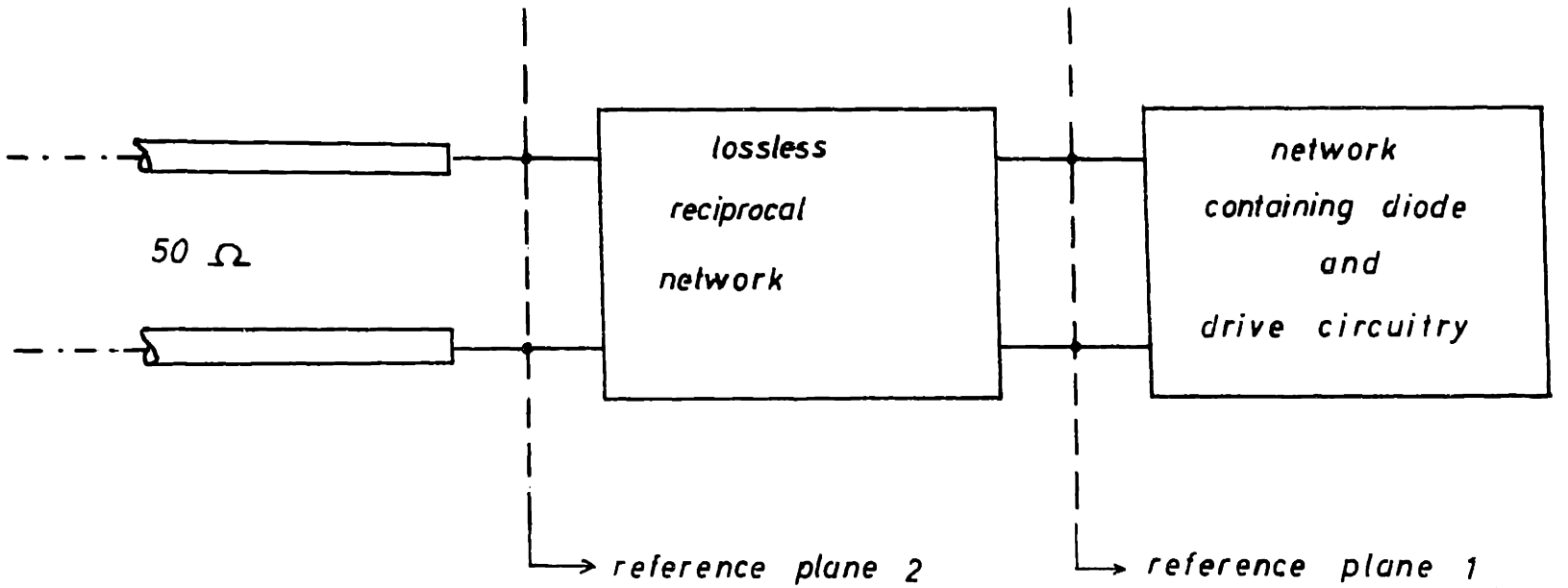

Fig. 1. Two state reflection-type modulator.

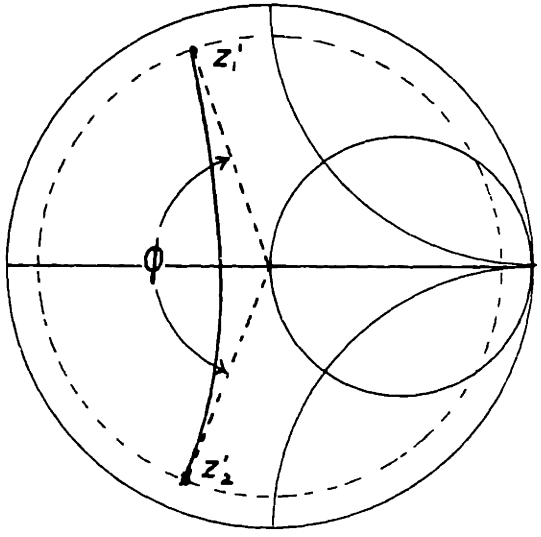

RP-2

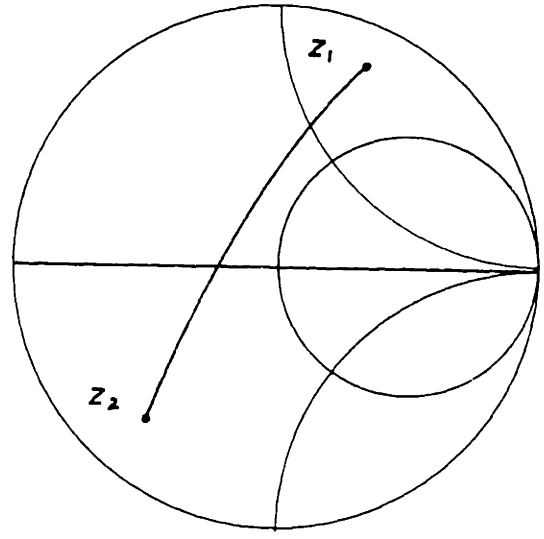

RP-1

Fig. 2. Diode impedances at RP-1 and RP-2.

According to (2), Γ_1' and Γ_2' will give

$$\left|\frac{z_1' - 1}{z_1' + 1}\right| = \left|\frac{z_2' - 1}{z_2' + 1}\right|, \tag{3}$$

where z_1' and z_2' are the normalized ON-OFF impedances at RP-2.

The lossless-reciprocal network must perform a simultaneous mapping of the diode impedances at RP-1 to a new position on the Γ-plane, characterized by (3) and (4)

$$\Gamma_1' = \left|\frac{z_1' - 1}{z_1' + 1}\right|; \qquad \Gamma_2' = \left|\frac{z_2' - 1}{z_2' + 1}\right| e^{j\phi}, \tag{4}$$

where ϕ is a specified angle of modulation.

III. GEOMETRICAL INTERPRETATION OF SIMULTANEOUS MAPPING OF TWO ARBITRARY IMPEDANCES

Following the analysis of the 0-180° phase modulator reported elsewhere,[11] we shall try to convert the double-valued impedance mapping to a single-valued impedance mapping on the hyperbolic plane, by means of a geometrical interpretation of the problem. Having (3) as a constraint, the single-valued equivalent matching impedance $z_\phi = r_\phi + jx_\phi$, which after matching to a 50 Ω line produces (3), will be located on the perpendicular bisector to the hyperbolic straight line through z_1 and z_2, the ON-OFF diode impedances at RP-1 (Fig. 3). [Note that z_ϕ, the impedance that we call the "equivalent matching impedance," does not in general belong to the impedance locus of the diode as a function of bias, and is a mathematical artifice.]

Since in non-Euclidean geometry a transformation through a lossless reciprocal network constitutes a rigid displacement, the operation of matching the equivalent matching impedance to a 50 Ω line is equivalent to moving impedances z_1 and z_2 to z_1' and z_2', respectively (Fig. 2). Under a lossless transformation, angles are preserved; hence, we can work in the geometrical model of Fig. 3 to calculate the coordinates of z_ϕ for a given angle ϕ and

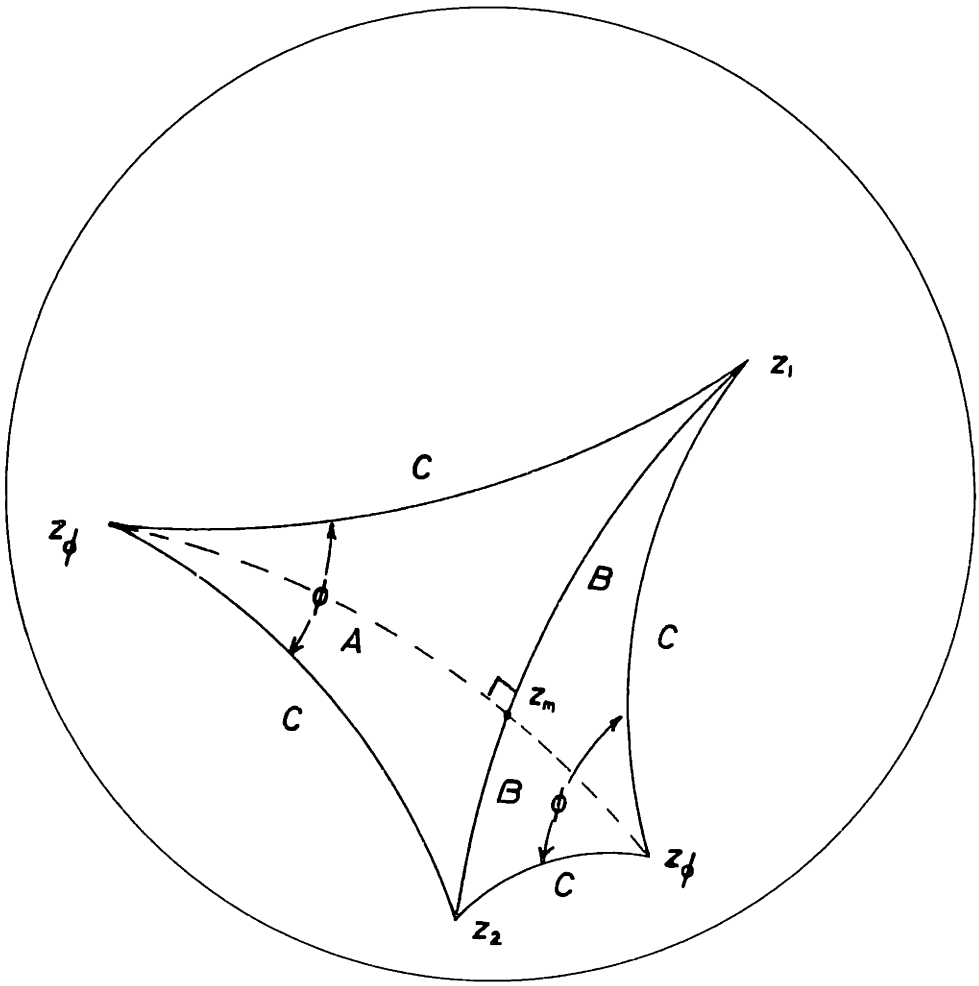

Fig. 3. Matching impedance Z_ϕ and diode impedances on the Γ-plane.

impedances z_1 and z_2. It is seen from Fig. 3 that for angles other than 180°, two solutions for z_ϕ can be found. For $\phi = 180°$, there is a unique solution, z_m, located in the non-Euclidean middle point of the hyperbolic straight line through z_1, z_2.

3.1 HYPERBOLIC DISTANCES IN TERMS OF THE QUALITY FACTOR $\hat{Q}$

By definition, the triangles inside the regular polygon are congruent. This means that it is enough to solve one triangle to obtain results for the others.

Let us take the triangle z_ϕ, z_m, z_1 and call its sides A, B, C representing the hyperbolic distances between z_ϕ-z_m, z_m-z_1, and z_1-z_ϕ, respectively.

To solve a triangle in non-Euclidean hyperbolic geometry as in Euclidean geometry at least 3 quantities are needed. Since we know only two, the hyperbolic distance between z_1 and z_m, and the angle $\phi/2$ which is one-half the modulation angle, we can express the side, C, in terms of these two quantities. The hyperbolic distance between z_1 and z_2 in terms of $\hat{Q}$ is given (see Appendix A) by

$$\delta = \log \left| \frac{(\hat{Q}^2 + 4)^{1/2} + \hat{Q}}{(\hat{Q}^2 + 4)^{1/2} - \hat{Q}} \right| . \qquad (5)$$

Side B is one-half of this distance; hence,

$$B = \frac{1}{2} \log \left[\frac{(\hat{Q}^2 + 4)^{1/2} + \hat{Q}}{(\hat{Q}^2 + 4)^{1/2} - \hat{Q}} \right]. \tag{6}$$

Equation 6 can be expressed as

$$\hat{Q} = 2 \sinh B. \tag{7}$$

If we define $\hat{Q}_\phi$ as the $\hat{Q}$ between z_1 and z_ϕ, we can express the hyperbolic distance C as

$$C = \log \left[\frac{(\hat{Q}_\phi^2 + 4)^{1/2} + \hat{Q}_\phi}{(\hat{Q}_\phi^2 + 4)^{1/2} - \hat{Q}_\phi} \right], \tag{8}$$

or equivalently

$$\hat{Q}_\phi = 2 \sinh \frac{C}{2}. \tag{9}$$

Equation 9 can also be expressed as

$$\sinh C = \left[\left(\frac{\hat{Q}_\phi^2}{2} + 1 \right)^2 - 1 \right]^{1/2}. \tag{10}$$

For the triangle, z_ϕ, z_m, z_1, in non-Euclidean hyperbolic trigonometry the following expression[10] holds:

$$\sin \frac{\phi}{2} = \frac{\sinh B}{\sinh C}. \tag{11}$$

Introducing (7) and (10) in (11), we get

$$\sin \frac{\phi}{2} = \frac{\frac{\hat{Q}^2}{2}}{\left| \left(\frac{\hat{Q}_\phi^2}{2} + 1 \right)^2 - 1 \right|^{1/2}}. \qquad (12)$$

Equation 12 can be written more conveniently

$$\hat{Q}_\phi = \left[2 \left| \sqrt{\frac{\hat{Q}^2}{2(1 - \cos\phi)} + 1} - 1 \right| \right]^{1/2}. \qquad (13)$$

$\hat{Q}_\phi$ can be regarded as a measure of the separation of the equivalent matching impedance from the ON-OFF impedances of the diode for a given modulation angle. Hence, for a given diode and phase angle between the reflection coefficients at RP-2 (Fig. 2), $\hat{Q}_\phi$ is known and unique.

Equation 13 is plotted in Fig. 4, for ϕ = 45°, 90°, 135°, 180°. It is important to note that $\hat{Q}_\phi$ for ϕ = 135° and 180° is almost the same, which indicates that the implementation must be accurate to achieve a given angle greater than 135°.

3.2 COORDINATES OF THE EQUIVALENT MATCHING IMPEDANCE

Since the hyperbolic distance between z_ϕ and z_2 is also equal to C (Fig. 3), $\hat{Q}_\phi$ is also given by (13). This

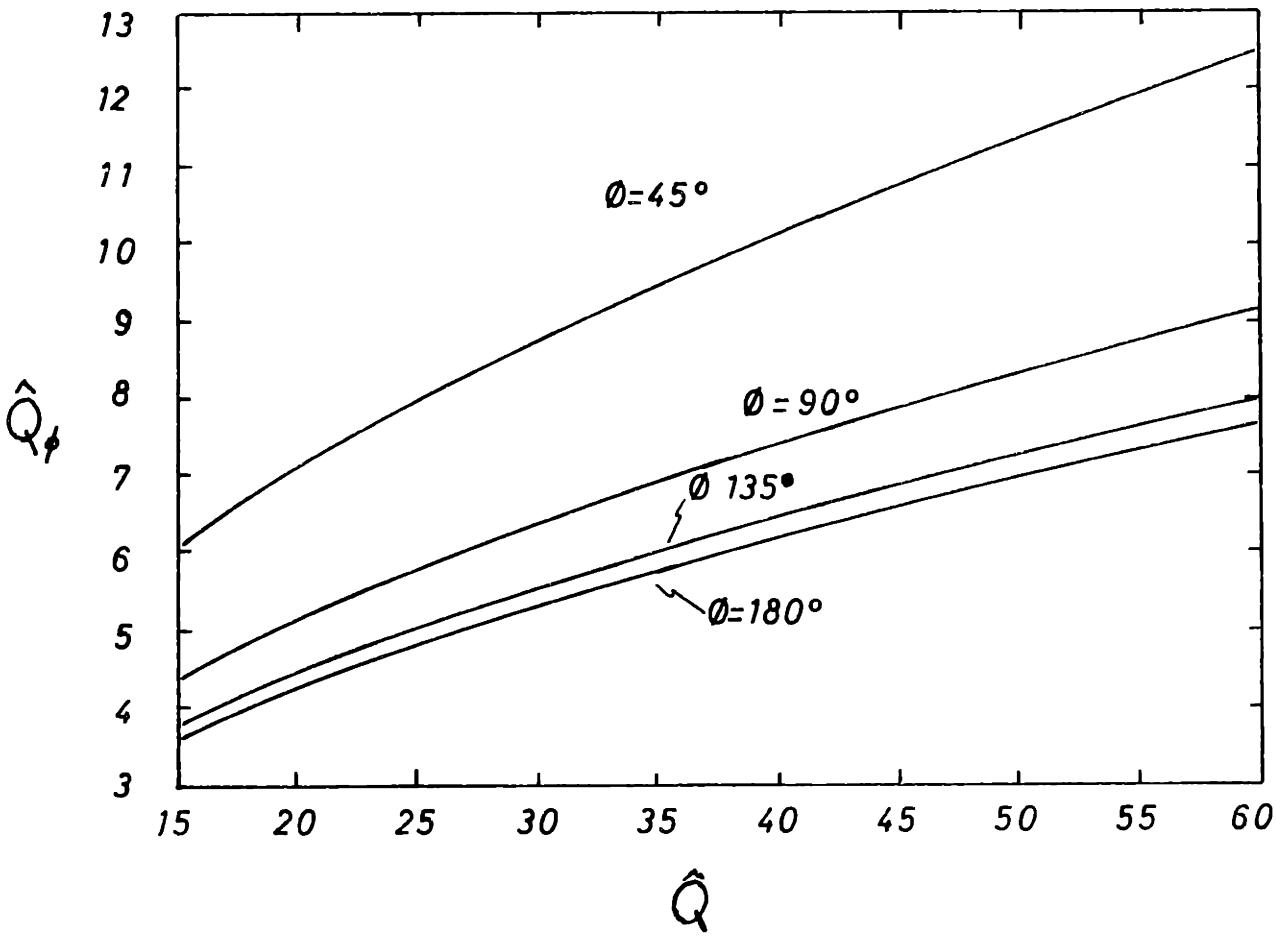

Fig. 4. Quality factor $\hat{Q}$ vs. $\hat{Q}_\phi$ for different angles of modulation.

fact permits us to write two simultaneous equations in r_ϕ and x_ϕ (real and imaginary parts of z_ϕ) as a function of z_1, z_2, and $\hat{Q}_\phi$.

$$\frac{\left|(r_1-r_\phi)^2 + (x_1-x_\phi)^2\right|^{1/2}}{(r_1 r_\phi)^{1/2}} = \hat{Q}_\phi$$

$$\frac{\left|(r_2-r_\phi)^2 + (x_2-x_\phi)^2\right|^{1/2}}{(r_2 r_\phi)^{1/2}} = \hat{Q}_\phi. \tag{14}$$

Solving (14), we get

$$x_\phi = \frac{-b \pm \sqrt{b^2 - 4ac}}{2a}$$

$$r_\phi = \frac{-k - 2x_\phi(x_1 - x_2)}{k_1}, \tag{15}$$

where

$$a = \frac{4}{k_1^2}(x_1 - x_2)^2 + 1$$

$$b = \frac{2(x_1 - x_2)r_1}{(r_1 - r_2)} - 2x_1 - \frac{4k}{k_1^2}(x_1 - x_2)$$

$$c = r_1^2 + x_1^2 - \frac{k}{k_1} r_1(\hat{Q}^2 + 2) + \left(\frac{k}{k_1}\right)^2 \tag{16}$$

$$k = r_1^2 - r_2^2 + x_1^2 - x_2^2$$

$$k_1 = (2 - \hat{Q}^2)(r_1 - r_2).$$

3.3 PHYSICAL REALIZATION OF THE MATCHING NETWORK

Having determined $z_\phi = r_\phi + jx_\phi$, we need to match this impedance to a 50 Ω line. This operation will move z_ϕ to the center of the chart and transform z_1 and z_2 into z_1' and z_2', two symmetric impedances with respect to the center of the Γ-plane (Fig. 2). A fixed-length matching network[12] or a single line of variable length have been previously described[11] and the selection of the network will depend on the value of z_ϕ and the kind of implementation. For high angles of modulation in general there is no difficulty in matching z_ϕ to a 50 Ω line, since z_ϕ is located near the center of the chart. For low angles of modulation, z_ϕ moves the limb of the chart forward and so serious problems can arise in implementation.

IV. LIMITATIONS OF PRACTICAL MODELS

4.1 MAXIMUM AND MINIMUM ANGLES OF MODULATION

From (13) we see that the maximum modulation angle $\phi = 180°$ can easily be achieved because there are no singularities for that particular value of ϕ. In fact, this value of modulation angle, in the majority of the cases, yields values of z_ϕ that can easily be matched to a 50 Ω line. A typical switching diode measured between 2 GHz and 3 GHz gave the values of z_ϕ plotted in Fig. 5. For very low values of ϕ, (13) goes to infinity, and in the limit when ϕ approaches zero (13) is approximated by

$$\hat{Q}_\phi \approx \frac{\hat{Q}^{1/2}}{\sin \phi/2} \approx \frac{2(\hat{Q})^{1/2}}{\phi}. \qquad (17)$$

Actually this theoretical lower limit of ϕ is seldom reached because for even greater values of ϕ, when (17) does not hold, $\hat{Q}_\phi$ is so high that the resultant equivalent matching impedance z_ϕ lies outside of the range of impedance that can be matched to a 50 Ω line. On the other hand, if the value of normalization impedance can be changed freely, the lower limit $\phi = 0°$ is achieved only for $\hat{Q} = 0$.

4.2 LOSSES IN A TWO-STATE REFLECTION-TYPE MODULATOR TWO-PORT IMBEDDED

Since (2) is a constraint, the losses are the same in both states given by

$$1 - |\Gamma_1'|^2 = 1 - |\Gamma_2'|^2. \tag{18}$$

The reflection coefficient in terms of $\hat{Q}_\phi$ (see Appendix A) is

$$|\Gamma_1'| = |\Gamma_2'| = \frac{\hat{Q}_\phi}{\sqrt{\hat{Q}_\phi + 4}}, \tag{19}$$

which expresses the magnitude of the reflection coefficients at RP-2 (Fig. 2), in terms of $\hat{Q}_\phi$, defined in (13).

Hence the losses are

$$\frac{4}{\hat{Q}_\phi^2 + 4}, \tag{20}$$

or more explicitly, by introducing (13) in (20)

$$\frac{2}{\left|\frac{\hat{Q}^2}{2(1 - \cos\phi)} + 1\right|^{1/2} + 1}. \tag{21}$$

Expression (21) is equivalent to Kurokawa and Schlosser's, but slightly more compact and written in terms of the full angle of modulation.

4.3 FREQUENCY SENSITIVITY OF THE EQUIVALENT MATCHING IMPEDANCE

When the frequency changes, the ON-OFF diode impedances at RP-1 (Fig. 1), move on the Γ-plane, since the real and imaginary parts of the forward and reverse bias diode impedances are frequency-dependent.[13] Strictly speaking, if an optimum match is needed, we should find a model of the locus of z_ϕ vs. frequency on the Γ-plane, and then design the broadband matching network by means of Fano's[14] equations.

The ON-OFF impedances of several diodes were measured as a function of frequency, and we found that both impedances moved clockwise with positive increments of frequency. The degree of frequency sensitivity of z_ϕ is inversely proportional to the value of phase modulation, as we might expect from a graphical analysis (Fig. 3). A plot of z_ϕ vs. frequency for several modulation angles is shown in Fig. 5. It is evident that the real part of z_ϕ was practically constant in the whole frequency range in which the diodes were measured. This behavior is predictable if the diode has ON-OFF impedances located nearly in quadrature with respect to the real axis of the Smith Chart.

From Fig. 3 it can be seen that if the hyperbolic straight line through z_1 and z_2 rotates on the Γ-plane

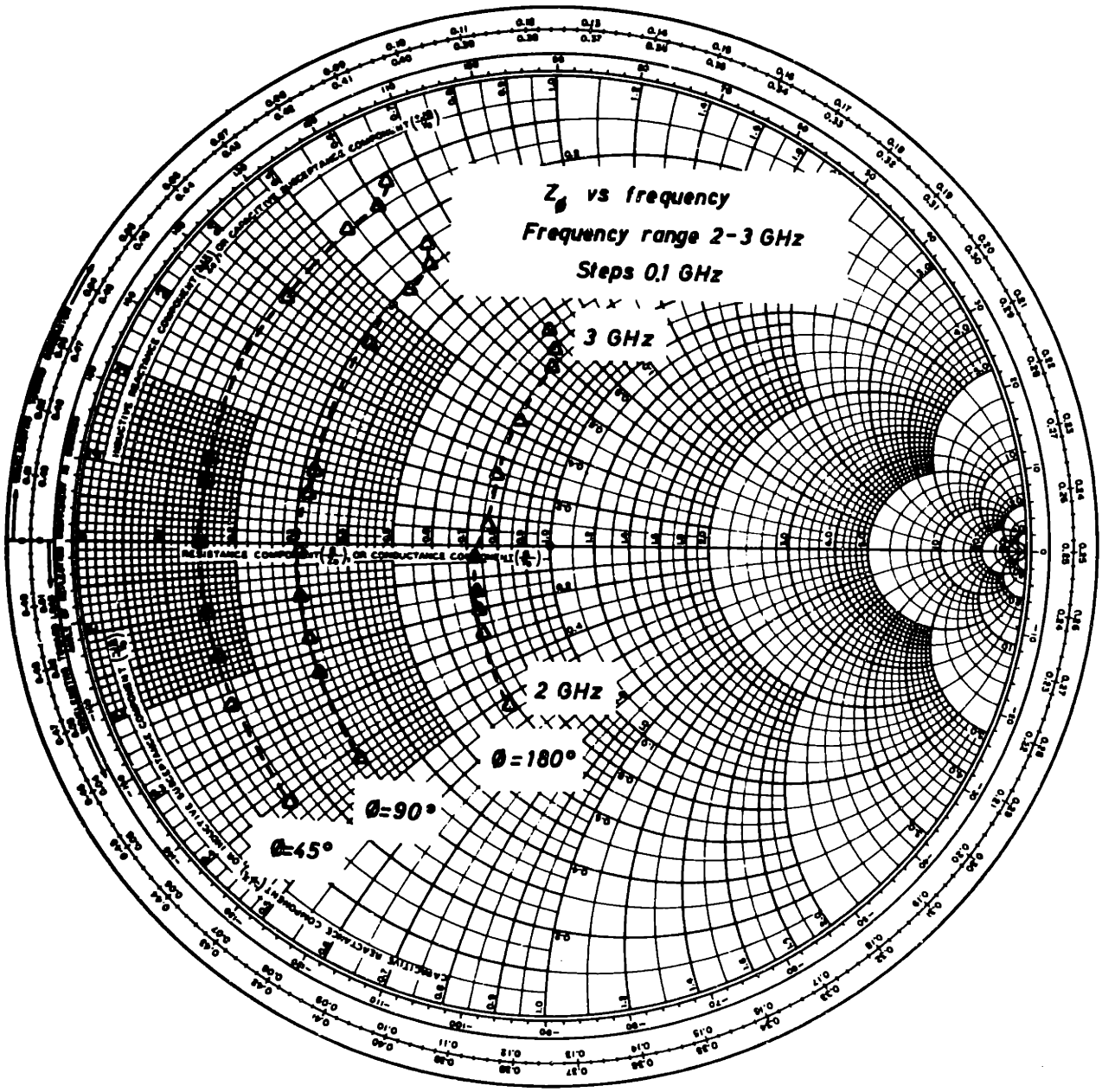
Z_ϕ vs frequency
Frequency range 2-3 GHz
Steps 0.1 GHz
3 GHz
2 GHz
Ø=180°
Ø=90°
Ø=45°

Fig. 5

with a frequency change, the vertex, z_ϕ, of the triangle z_ϕ, z_1, z_2 will describe an arc inversely proportional to the angle ϕ.

V. BROADBANDING TECHNIQUES

When the frequency band is moderated (less than 10% of midband frequency) the following procedure can be used as a first approximation of broadband operation. From Fig. 5, for a certain frequency z_ϕ is resistive. This leads to a straightforward design of the matching network. Since we are interested in broadband operation, a broadband matching network can be used to match the real part of z_ϕ to a 50 Ω line. The perfect match that produces the desired angle of modulation occurs only at the frequency at which z_ϕ is resistive. At greater or lower frequencies, z_ϕ is complex, and the match is not perfect,[14] which leads to a different angle of modulation. The bandwidth in this case is not defined, and depends on the permissible percent of error in the phase-modulation angle.

5.1 OPTIMUM DIODE CHARACTERISTICS FOR BROADBAND OPERATION

Referring to (15), we shall investigate the condition(s) needed to get x_ϕ equal to zero.

To simplify the analysis, we shall calculate the condition(s) for $\phi = 180°$, where $b^2 - 4ac$ in (15) is zero, since for this value of ϕ there is only one solution for z_ϕ. From (15) the only possibility for $x_\phi = 0$ is $b = 0$.

After some manipulation we find (Appendix B) that the condition is

$$\frac{x_1}{r_1} = - \frac{x_2}{r_2}. \qquad (22)$$

This indicates that the phase of the diode impedance in one state must be equal to the negative value of the phase impedance in the other state. This curious relation can be clarified by a graphical analysis on the hyperbolic plane.

5.2 GRAPHICAL ANALYSIS OF THE CONDITION FOR BROADBAND OPERATION

The loci of constant phase on the Smith Chart are arcs of circles through -1 and +1. This is evident if we consider that a locus of constant phase on the z-plane is a straight line from zero to infinity, since a bilinear transformation relates the z-plane to the Γ-plane, where straight lines map into circles , the circles must pass through -1 and +1 on the Γ-plane (Fig. 6).

Let us call h_1 and h_2 the hyperbolic distances from z_1 and z_2 (measured through perpendiculars) to the real axis of the Smith Chart. If z_1 and z_2 lie on constant-phase circles of the same absolute value, we claim that

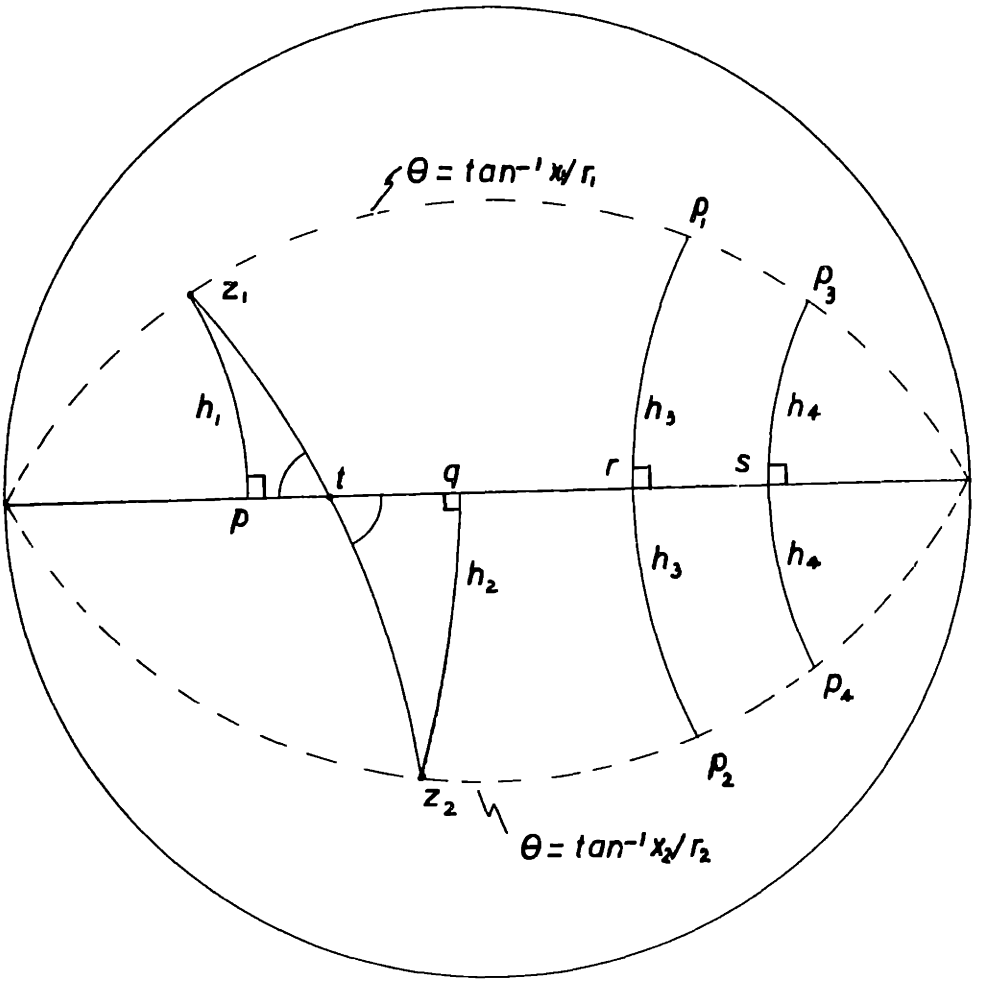

Fig. 6. Geometrical interpretation of condition for broadband operation.

$h_1=h_2$ and t the non-Euclidean middle point of the hyperbolic straight line through z_1 and z_2 will be located on the real axis of the Smith Chart.

To prove the last statement, we need only show that $h_1 = h_2$ and also are equal to any other hyperbolic distance measured through a perpendicular to the real axis of the Smith Chart, from any of the two circles of the same absolute phase value.

To do this, we draw two more hyperbolic straight lines, perpendicular to the real axis of the Smith Chart (Fig. 6). We call

$$p_1 r = p_2 r = h_3$$

and (23)

$$p_3 s = p_4 s = h_4$$

where h_3 and h_4 are the hyperbolic distances.

We need to prove that $h_3 = h_4$. Let

$$p_1 = r_a + jx_a \qquad p_3 = C(r_a + jx_a)$$

(24)

$$p_2 = r_a - jx_a \qquad p_4 = C(r_a - jx_a),$$

where C is a real constant.

Since $\hat{Q}$ is an invariant function of the hyperbolic distance (see Appendix A), it is enough to prove

$$\hat{Q}_{p_1p_2} = \hat{Q}_{p_3p_4}. \tag{25}$$

Substituting (24) in (25) gives

$$2\,\frac{x_a}{r_a} = 2\,\frac{x_a}{r_a}, \tag{26}$$

or conversely

$$h_3 = h_4, \tag{27}$$

and consequently

$$h_1 = h_2. \tag{28}$$

To prove that t lies on the real axis of the Γ-plane, the arguments of Euclidean geometry also apply. The triangles z_1, p, t and z_2, q, t are congruent, since they have two angles and one side of the same value. Hence, the hypotenuse and the sides of both on the real axis have the same values, and consequently t is **the non-Euclidean** middle point of the hyperbolic straight lines through z_1, z_2 and p, q, respectively.

For $\phi \neq 180°$ condition (22) is no longer valid, but from (15) and (16) a similar analysis can be made to get an analytical expression for the condition(s) needed for $x_\phi = 0$.

This involved operation can be avoided, if the diode not only has the ON-OFF impedances related by (22) but also the reactive part of the ON-OFF impedances approaching the same absolute value. If this situation occurs at a given frequency, the perpendicular bisector to the hyperbolic straight line through z_1, z_2 will approach a straight line in the Euclidean sense, overlapping the real axis of the Smith Chart leading to a z_ϕ resistive for all values of ϕ.

5.3 THEORETICAL DETERMINATION OF THE OPTIMUM FREQUENCY OF OPERATION FOR $\phi = 180°$

The following expressions are valid for reverse and forward bias conditions in a switching diode.[13]

$$Y_r = \frac{(\frac{1}{R_s})(\frac{f}{f_{co}})^2}{\left|1-(\frac{f}{f_r})^2\right|^2} + j\omega\left|\frac{C_j}{1-(\frac{f}{f_r})^2} + C_c\right| \tag{29}$$

$$Y_f = \frac{R_f}{R_f^2 + (\omega L_s)^2} + j\omega\left|C_c - \frac{\omega L_s}{R_f^2 + (\omega L_s)^2}\right|,$$

where Y_r is the reverse-bias admittance, Y_f the forward bias admittance, f_{co} the diode cutoff frequency, and f_r the reverse-bias series resonant frequency.

The condition for zero reactance ($x_\phi = 0$) is

$$\frac{r_2}{r_1} = -\frac{x_2}{x_1}. \tag{30}$$

From (29)

$$r_2 = R_e\left(\frac{1}{Y_f}\right) = \frac{\dfrac{R_f}{[R_f^2 + (\omega L_s)^2]}}{\dfrac{R_f^2}{[R_f^2 + (\omega L_s)^2]^2} + \left|\omega C_c[R_f^2 + (\omega L_s)^2] - \omega L_s\right|^2}$$

$$r_1 = R_e\left(\frac{1}{Y_r}\right) = \frac{\dfrac{1/R_s\,(f/f_{co})^2}{[1 - (\frac{f}{f_r})^2]^2}}{\left(\dfrac{\frac{1}{R_s}\,(\frac{f}{f_{co}})^2}{[1 - (\frac{f}{f_r})^2]^2}\right)^2 + \omega^2\left|\dfrac{C_j + C_c[1 - (\frac{f}{f_r})^2]}{1 - (\frac{f}{f_r})^2}\right|}$$

$$I_m\left(\frac{1}{Y_f}\right) = x_2 = \frac{\dfrac{\omega C_c[R_f^2 + (\omega L_s)^2] - \omega L_s}{R_f^2 + (\omega L_s)^2}}{\dfrac{R_f^2}{[R_f^2 + (\omega L_s)^2]^2} + \left|\omega C_c[R_f^2 + (\omega L_s)^2] - \omega L_s\right|^2} \tag{31}$$

$$x_1 = I_m\left(\frac{1}{Y_r}\right) = \frac{-\omega\left|\dfrac{C_j + C_c[1 - (\frac{f}{f_r})^2]}{1 - (\frac{f}{f_r})^2}\right|}{\left(\dfrac{\frac{1}{R_s}\,(\frac{f}{f_{co}})^2}{[1 - (\frac{f}{f_r})^2]^2}\right)^2 + \omega^2\left|\dfrac{C_j + C_c[1 - (\frac{f}{f_r})^2]}{1 - (f/f_r)^2}\right|}$$

Substituting (31) in (30), we get

$$\frac{R_s R_f [1 - (\frac{f}{f_r})^2]}{(\frac{f}{f_{co}})^2} = \frac{C_c[R_f^2 + (\omega L_s)^2] - L_s}{C_j + C_c[1 - (\frac{f}{f_r})^2]}. \qquad (32)$$

With the approximation $f^2 L_s >> C_c R_f^2 f^2$, and by replacing

$$f_{co} = \frac{1}{4\pi^2 R_s^2 C_j^2}$$

and (33)

$$L_s C_j = \frac{1}{4\pi^2 f_r^2}$$

in (32), we get

$$A(\frac{f}{f_r})^4 + B(\frac{f}{f_r})^2 + C = 0, \qquad (34)$$

where

$$A = R_s R_f C_c - R_s^2 C_c$$

$$B = R_s R_f (2C_c - C_j) - R_s^2 C_j$$

$$C = R_s R_f (C_j + C_c)$$

The mounting technique will determine the value of the parallel capacitance C_c, and consequently will be an important factor in the determination of the frequency in which the equivalent matching impedance Z_ϕ is resistive.

VI. FOUR-STATE REFLECTION-TYPE MODULATOR, THREE-PORT IMBEDDED

A three-port lossless-reciprocal network is characterized by the determinant

$$\begin{vmatrix} z_{11} - z_{in} & z_{12} & z_{13} \\ z_{21} & z_{22} - z_{2n} & z_{23} \\ z_{31} & z_{32} & z_{33} - z_{3n} \end{vmatrix} = 0, \quad (35)$$

where n = 1,2 indicates the state of the load impedances at ports 2 and 3 (Fig. 7).

From (35)

$$z_{in} = f(z_{3n}, z_{2n}). \quad (36)$$

Since we are interested in the phase of the reflection coefficient, we get

$$\Gamma_1 = \frac{z_{in} - z_o}{z_{in} + z_o}. \quad (37)$$

Normalizing all impedance values to $z_o = 1\ \Omega$ and assuming z_{in} imaginary, we get

$$\angle \Gamma_1 = \theta = -2 \tan^{-1} z_{in}. \quad (38)$$

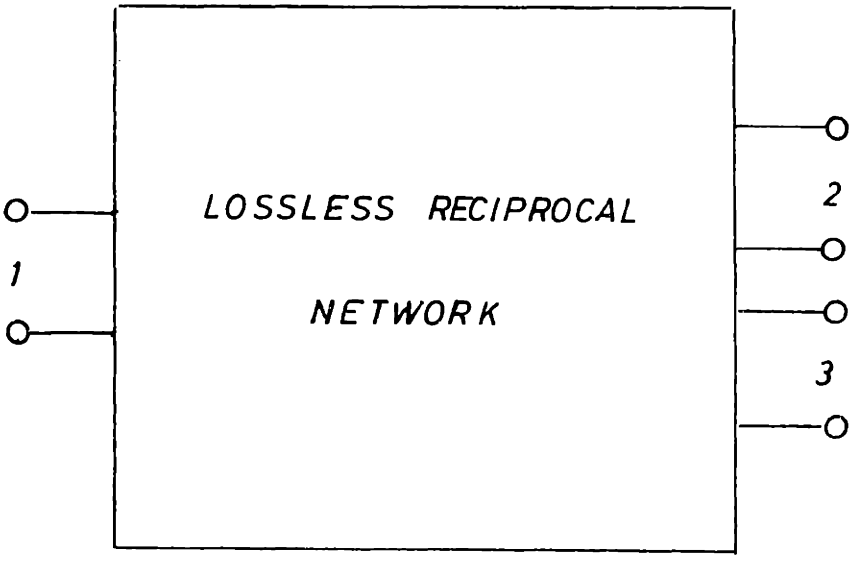

Fig. 7. A general 3-part lossless-reciprocal network.

Now two questions arise: What characteristics should have z_{in} to get four point equal spaced?, and under what conditions can z_{in} be imaginary?

6.1 SYNTHESIS OF z_{in}

A plot of (38) is shown in Fig. 8. It can be seen that the only possibility of getting four points equally spaced is to have z_{in} formed by two terms, each one quantized in two states. Each state should be symmetrical with respect to the origin. Since we assumed a z_{in} imaginary, each term of z_{in} will have a value and its complex conjugate. The assumption of z_{in} imaginary is now more evident.

A switching diode has its ON-OFF characteristics almost on the limb of the Smith Chart, therefore in this case, the assumption of an imaginary impedance is justified. If we make

$$z_{in} = \sum \text{diode impedances}, \tag{39}$$

in (38), then (38) will be justified.

There are many circuits that can satisfy (39); the circuits presented here represent only one way of realizing a 4S-RM-3PI network and not necessarily the best.

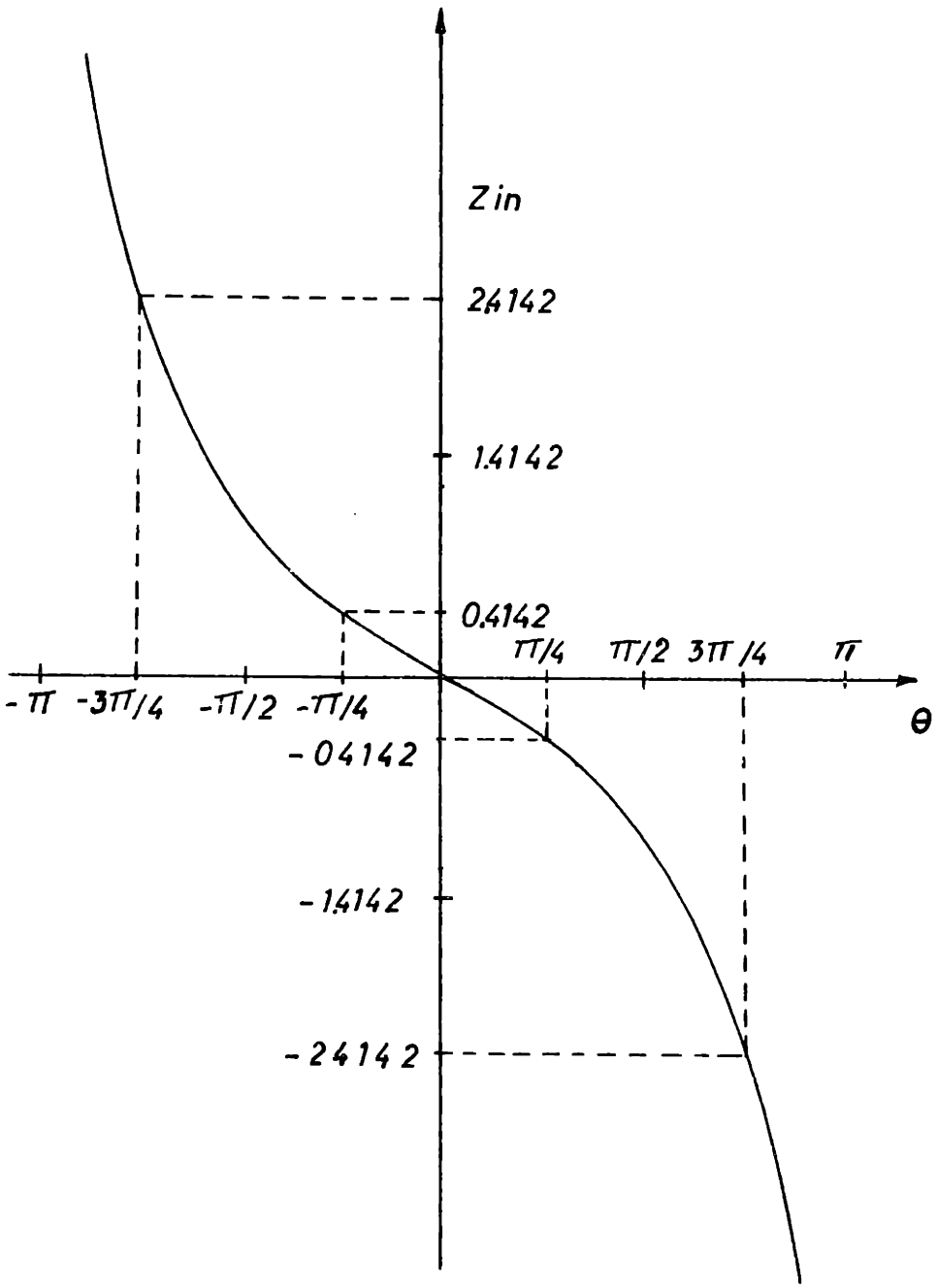

Fig. 8. Values of zin for 4 equally spaced states.

For simplicity, we choose a TEM model of the Y-junction (Fig. 9).

6.2 VALUES OF PORT IMPEDANCES IN A 4S-RM-3PI NETWORK

Let z_a and z_b represent the 2-state impedances that we will get from a 2S-RM-2PI (Fig. 9). We want at terminals 2-2' a reflection coefficient quantized in four states, and equal spaced on the Γ-plane.

The expression for the angle of Γ at port 2-2' is easily calculated in terms of the impedance at 1-1'.

$$z_{1-1'} = \frac{kz_o}{z_a + z_b}$$

$$z_{2-2'} = \frac{z_a + z_b}{k}. \qquad (40)$$

Therefore

$$\Gamma_{2-2'} = \frac{\frac{z_a + z_b}{k} - z_o}{\frac{z_a + z_b}{k} + z_o} \qquad (41)$$

Normalizing all the impedance values with respect to z_o, we get:

$$\angle \Gamma_{2-2'} = = -2 \tan^{-1} \frac{z_a + z_b}{k} \qquad (42)$$

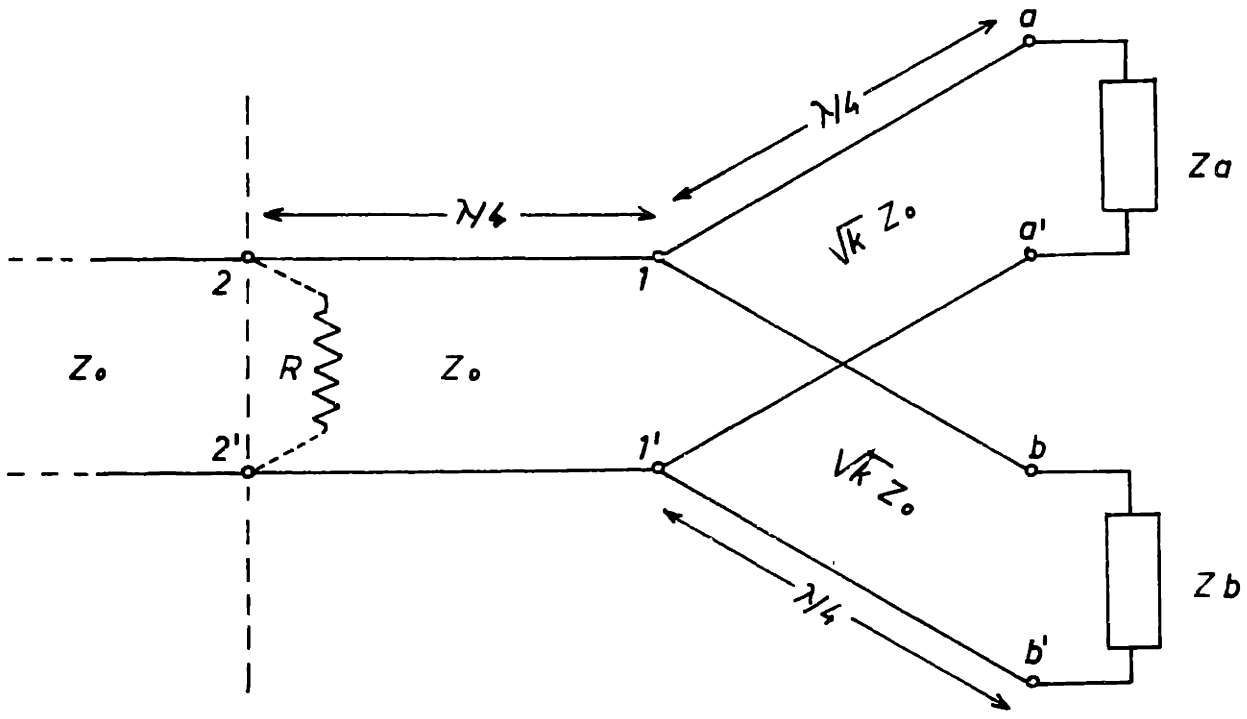

Fig. 9. Symmetric Junction.

We assume that z_a and z_b are imaginary, which is a reasonable assumption for switching diodes. A plot of (39) is shown in Fig. 8. Inspection of (39) shows that the only possibility of getting 4 states equally spaced is to choose z_a and z_b in such a way that a change of state in z_a and z_b produces equal increments in $\frac{z_a + z_b}{k}$. The values of $\frac{z_a + z_b}{k}$ in Fig. 8 are the unique values that permit 4 states equally spaced.

These four states are

$$\frac{z_{a_1} + z_{b_1}}{k} = j2.4142$$

$$\frac{z_{a_2} + z_{b_1}}{k} = -j0.4142$$

$$\frac{z_{a_1} + z_{b_2}}{k} = j0.4142 \qquad (43)$$

$$\frac{z_{a_2} + z_{b_2}}{k} = -j2.4142.$$

The values of z_a and z_b are

$$\frac{z_{a_1}}{k} = j1.4142; \quad \frac{z_{b_1}}{k} = j$$
$$\frac{z_{a_2}}{k} = j1.4142; \quad \frac{z_{b_2}}{k} = -j. \qquad (44)$$

6.3 ANGLES OF REFLECTION COEFFICIENTS AT PORTS a-a' & b-b'

Since we obtain z_a and z_b from a 2S-RM-2PI network, it is more convenient to express (41) in terms of the modulation angles at ports a-a' and b-b'.

To illustrate the procedure, take a value of k = 2. Then

$$z_{a_1} = j2.8284; \quad z_{b_1} = j2$$
$$z_{a_2} = -j2.8284; \quad z_{b_2} = -j2. \tag{45}$$

Hence

$$\Gamma_{a_1} = \frac{j2.8284 - 1}{j2.8284 + 1}$$

$$\angle \Gamma_{a_1} = \theta_{a_1} = -2 \tan^{-1} 2.8284$$

$$\theta_{a_1} = -141.0576°,$$

and consequently $\theta_{a_2} = +141.0576°$.

Following the same procedure, at the other port we get $\theta_{b_1} = -126.8699$ and $\theta_{b_2} = +126.8699$.

Since our equations for the design of 2S-RM-2PI network are in terms of the full angle of modulation, from the

last values we get

$$\phi_a = \theta_{a_2} - \theta_{a_1} = 77.8848°$$

and

$$\phi_b = \theta_{b_2} - \theta_{b_1} = 106.2602°. \tag{46}$$

If we choose k = 1 in (44), we get a complete symmetrical junction. Following the preceding analysis, we get the following results:

$$\begin{aligned} \theta_{a_1} &= -109.471° \\ \theta_{a_2} &= +109.471° \\ \theta_{b_1} &= -90° \\ \theta_{b_2} &= +90°, \end{aligned} \tag{47}$$

and consequently the modulation angles of the 2S-RM-2PI network at ports a-a' and b-b' are

$$\begin{aligned} \phi_a &= 141.058° \\ \phi_b &= 180°. \end{aligned} \tag{48}$$

6.4 ASYMMETRICAL JUNCTION

A study of (39) and (40) indicates that for a sym-

metrical junction, regardless of the value of k, we shall never get the same conditions at ports a-a' and b-b' (Fig. 9).

Let us repeat the analysis for the asymmetrical junction of Fig. 10.

The angle of the reflection coefficient at 2-2' is

$$\theta = -2 \tan^{-1} \left(\frac{z_a}{k} + z_b\right). \tag{49}$$

We get 4 equations for the four states equally spaced, as in Eq. 43:

$$\begin{aligned}
\frac{z_{a_1}}{k} + z_{b_1} &= j2.4142 \\
\frac{z_{a_2}}{k} + z_{b_1} &= -j0.4142 \\
\frac{z_{a_1}}{k} + z_{b_2} &= j0.4142 \\
\frac{z_{a_2}}{k} + z_{b_2} &= -j2.4142.
\end{aligned} \tag{50}$$

After some manipulation we find that for $k = \frac{1}{\sqrt{2}}$

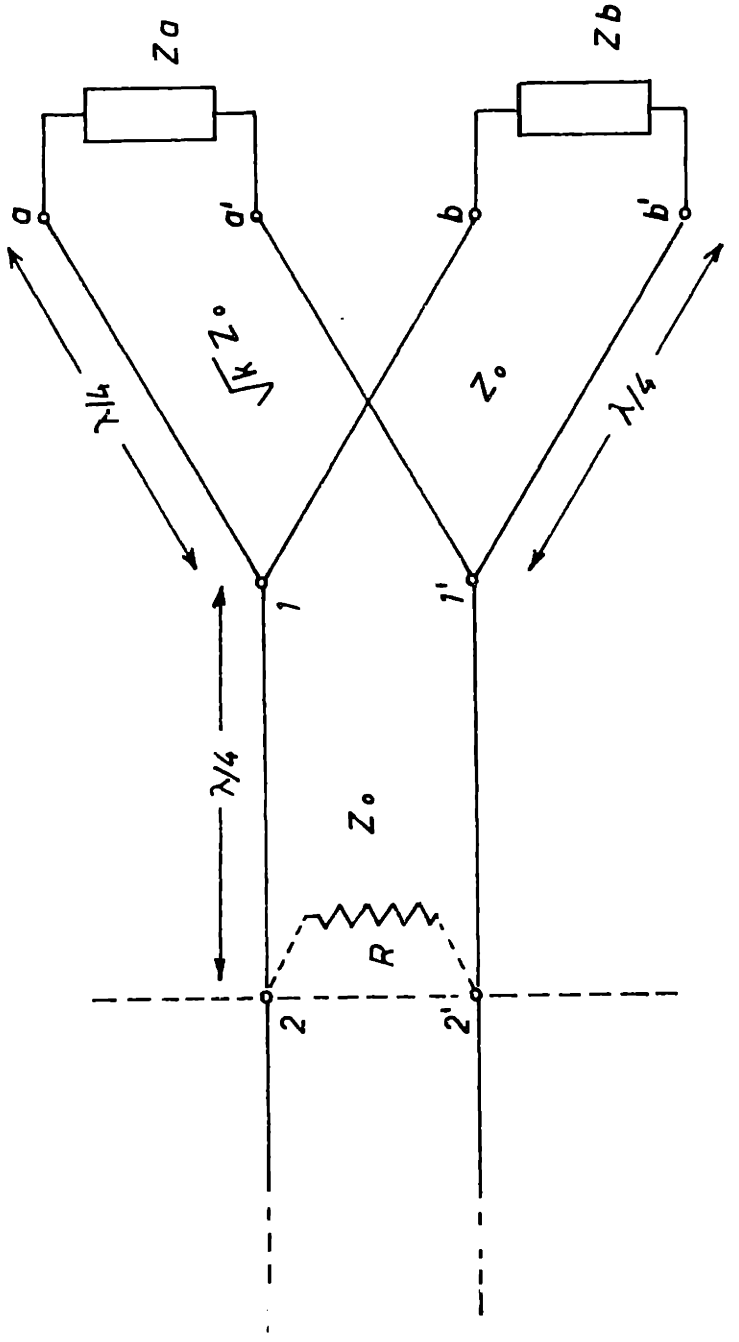

Fig. 10. Asymmetric Junction.

$$z_{a_1} = z_{b_1} = +j$$

$$z_{a_2} = z_{b_2} = -j \tag{51}$$

From (51), $\phi_a = \phi_b = 180°$, which tells us that 2 identical 2S-RM-2PI networks are needed to achieve 4 states equally spaced.

6.5 UNBALANCE OF THE REFLECTION COEFFICIENTS AT FOUR STATES

It has been shown[15] that with a lossless-reciprocal imbedding network, the losses at the four state cannot be equal, and a lossy element must be included to balance the amplitude of the reflection coefficients. For a series connection of two diodes, the equation which relates the resistor in parallel to the diode parameters is

$$R = \frac{1}{r_a + r_b} \tag{52}$$

where r_a and r_b are the resistances of the diodes. It is assumed that

$$r_a(1) = r_a(2)$$

and (53)

$$r_b(1) = r_b(2)$$

where (1) and (2) indicate the state of the diodes.

Since the networks that we have described have an input impedance equal to a series combination of the diode impedances, (52) can also be extended for all the networks with this characteristic. For the asymmetrical junction, we have

$$R = \frac{1}{\frac{r_a}{k} + r_b}. \tag{54}$$

For the symmetrical junction, we have

$$R = \frac{k}{r_a + r_b} \tag{55}$$

where R is the resistor in parallel with port 2-2' (Figs. 9 and 10).

We emphasize that condition (53), assumed by Schlosser[15], is one of the principal difficulties in the design of phase modulators, and to the best of our knowledge, no one has explained the method of achieving it. As we understand the problem, one possibility to get (53) is following the matching procedure discussed in the first section of this paper, and selecting properly the reference planes in order to get the ON-OFF impedances of the diode, the complex conjugates of each other. That means that the impedances of the diode must be located at symmetric positions with

respect to the real axis of the Smith Chart. This condition is also assumed in our synthesis procedure.

On the other hand, the circuits presented here have a gread advantage: they permit the selection of the modulation angles at ports a-a' and b-b' (Figs. 9 and 10) by a proper choice of the characteristic impedances of the lines.

6.6 BALANCED STATES WITH LOSSY ELEMENT

When a resistor is connected in parallel to a series connection of two diodes, the equivalent impedance can be approximated by[15]

$$z_{eq} = r + \frac{x^2}{R} + jx \tag{56}$$

where $r = r_a + r_b$ and $x = x_a + x_b$ are the series resistances and reactances of the diodes.

Condition (53) is also assumed. Before the resistor R is placed in parallel, the impedance of the series connection is

$$z = r + jx \tag{57}$$

and since r is constant, the locus of this impedance is a circle of constant resistance on the Smith Chart. Obviously

from Fig. 11, any four points on this circle will have a different magnitude of reflection coefficient. For points symmetric to the real axis of the Smith Chart, we will have two magnitudes of reflection coefficients, but never will it be possible to get four points completely symmetric with respect to the center of the Chart.

When a resistor in parallel is added, the real part of the equivalent impedance increases and, consequently, the four points move inward to the center of the Chart, to a new position. The new position can be determined approximately by this simple reasoning. The value of R depends on the diode resistances, since (52) is valid for any distribution of the states on the Smith Chart (see Appendix E). Suppose that two points are very close to the 180° position on the Chart where $x \to 0$. According to (56), the equivalent impedance will be practically the same as without the resistor R. In the limit where $x = 0$, R doesn't affect the equivalent impedance, and we conclude that the locus of the equivalent impedance will be a symmetric curve with center at the origin and tangential to the constant resistance circle at $x = 0$.

As we see from Fig. 11, the assumption of a circle like the locus of z_{eq} is appropriate, and is exact for angles of modulation close to 180° at ports a-a' and b-b'

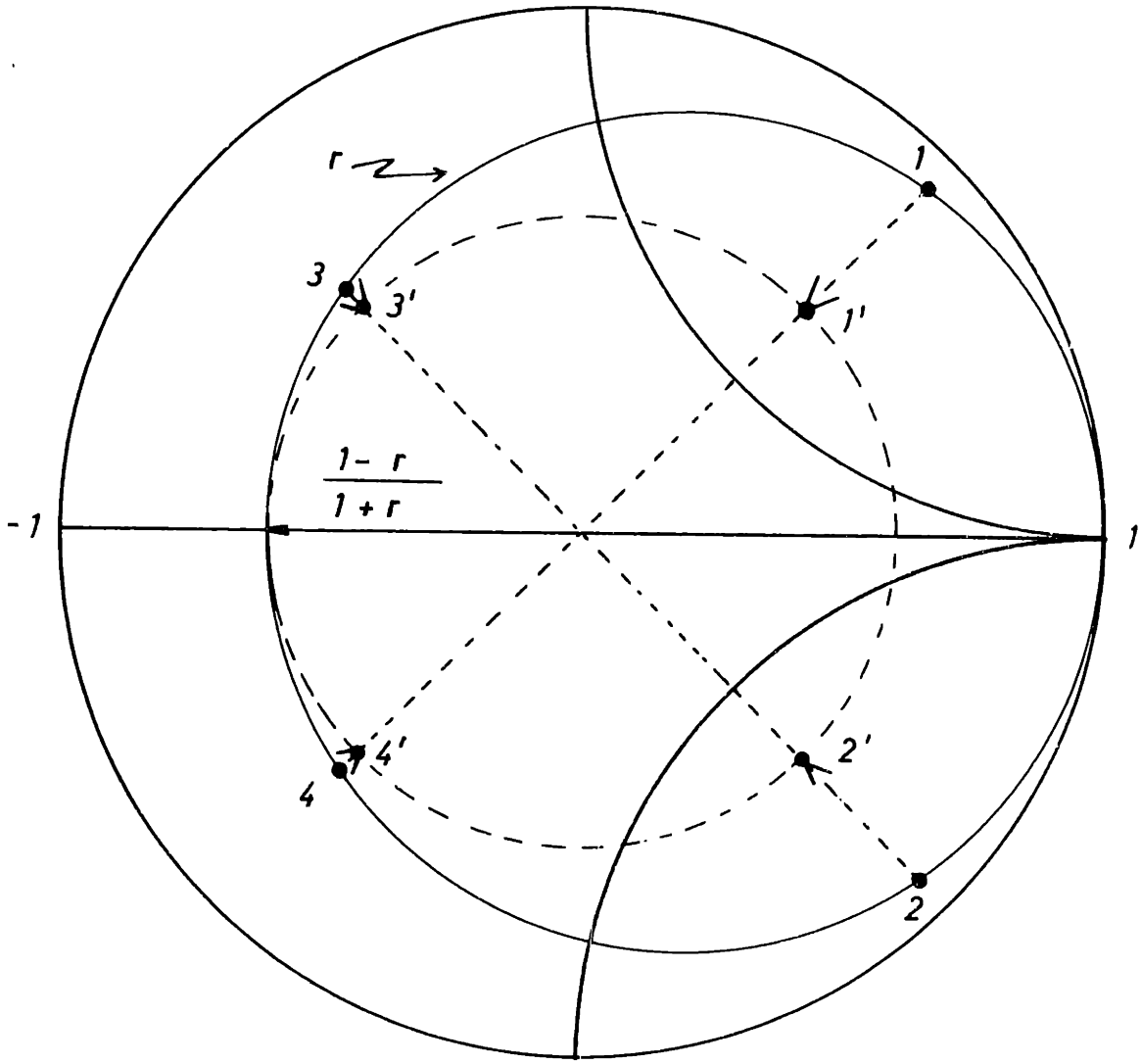

Fig. 11. Lossy transformation of unbalanced states.

of Figs. 9 and 10 (see Appendix E). On a scaled plot, the difference between points 3,4 and 3',4' is negligible and the circle assumed will be the actual locus of the four impedances. Therefore, the absolute value of the reflection coefficient will be

$$|\Gamma| = \frac{1 - r}{1 + r} \tag{58}$$

and the losses

$$1 - |\Gamma|^2. \tag{59}$$

6.7 LOSSES IN A FOUR-STATE, REFLECTION-TYPE MODULATOR, THREE-PORT IMBEDDED

According to (58) and (59), the losses are directly related to the resistance of the diodes, which determines the final locus of the four states on the Smith Chart. Therefore, we need an expression relating the resistance of the diodes to $\hat{Q}$ and ϕ, which are the design parameters of the 2S-RM-2PI at ports a-a' and b-b' (Figs. 9 and 10).

A locus of constant resistance on the Smith Chart is given by

$$r = \frac{1 - u^2 - v^2}{(1 - u)^2 + v^2} \tag{60}$$

where

$$u = |\Gamma| \cos \theta$$

and

$$v = |\Gamma| \sin \theta \tag{61}$$

are the real and imaginary parts of the reflection coefficient, and θ is one-half of the modulation angle, since it is assumed that the ON-OFF impedances are the complex conjugates of each other.

Substituting (61) in (60), we get

$$r = \frac{1 - |\Gamma|^2}{1 - 2\,|\Gamma| \cos \theta + |\Gamma|^2}. \tag{62}$$

$|\Gamma|$ can be expressed as (see Appendix A)

$$|\Gamma| = \frac{\hat{Q}_\phi}{\sqrt{\hat{Q}_\phi^2 + 4}}. \tag{63}$$

Substituting (63) in (62), we found

$$r = \frac{2}{\hat{Q}_\phi^2 + 2 - \hat{Q}_\phi (\hat{Q}_\phi^2 + 4)^{1/2} \cos \phi/2}. \tag{64}$$

Equation 64 is an exact expression for the resistance of the diodes when the ON-OFF impedances are the complex conjugates of each other, and can be used to evaluate the

the losses for a specific value of ϕ. However, a much simpler expression, and also exact, is the following, from (26)

$$r = \frac{2|x|}{\hat{Q}} \tag{65}$$

Equation 65 is a helpful relation which avoids a tedious evaluation of (64). On the other hand, it states that changes in $2|x|$ (or modulation angle at ports a-a' or b-b', Figs. 9 and 10) will produce changes in r of the same magnitude since $\hat{Q}$ is constant. Therefore, there is a maximum insertion loss limit that can be reached with a reciprocal network, since the characteristic impedances of the lines (Figs. 9 and 10) will not change the resistive part of the impedance at port 2-2'.

6.8 MAXIMUM LIMIT OF INSERTION LOSS IN A FOUR-STATE REFLECTION-TYPE MODULATOR

According to (44), the condition for equally spaced states in a four-state modulator is

$$z_a = \pm j1.4142$$

and

$$z_b = \pm j$$

Therefore, from (65), we get

$$r_a = \frac{2.8284}{\hat{Q}_a}$$

and

$$r_b = \frac{2}{\hat{Q}_b} \tag{66}$$

Hence, the total input resistance at port 2-2' Fig . 9 before R is connected in parallel is

$$r = \frac{2.8284}{\hat{Q}_a} + \frac{2}{\hat{Q}_b} \tag{67}$$

Substituting (67) in (58), we get the absolute value of the reflection coefficient, after R is connected in parallel to port 2-2'.

$$|\Gamma| = \frac{1 - \frac{2\sqrt{2}}{\hat{Q}_a} + \frac{2}{\hat{Q}_b}}{1 + \frac{2\sqrt{2}}{\hat{Q}_a} + \frac{2}{\hat{Q}_b}} \tag{68}$$

Equation 68 is a general equation for all 3-port networks discussed in this paper, independent of the characteristic impedances of the lines.

An evaluation of the losses in this reciprocal network shows that they are much similar to those predicted by Schlosser.[15] We must point out that the losses plotted in

Fig. 12 are the minimum losses that we can expect from a 4S-RM-3PI. A decrease in the angle of modulation at port a-a' and b-b' (Figs 9 and 10) actually reduce the losses (see Appendix E).

6.9 EIGHT-STATE REFLECTION-TYPE MODULATOR

A logical choice is a parallel combination of two 4S-RM-3PI networks which will give an 8S-RM-5PI network.

Let us analyze the circuit of Fig. 13. In terms of the 2S-RM-2PI impedances, the angle of the reflection coefficient at port 2-2' is

$$\angle \Gamma_{2-2'} = \theta = -2 \tan^{-1} \left[\left(\frac{z_a}{k_1} + \frac{z_b}{k_2} \right) + \left(\frac{z_c}{k_3} + \frac{z_d}{k_4} \right) \right] \qquad (69)$$

A plot of (69) is shown in Fig. 14. Following the same reasoning as for the 4S-RM-3PI network, each factor in (69) must take on the following values

$\frac{z_a}{k_1} + \frac{z_b}{k_2}$	$\frac{z_c}{k_3} + \frac{z_d}{k_4}$	θ
$\frac{m_3 + m_4}{2}$	$\frac{m_4 - m_3}{2}$	$-\theta_4$
$\frac{m_3 + m_4}{2}$	$\frac{m_3 - m_4}{2}$	$-\theta_3$

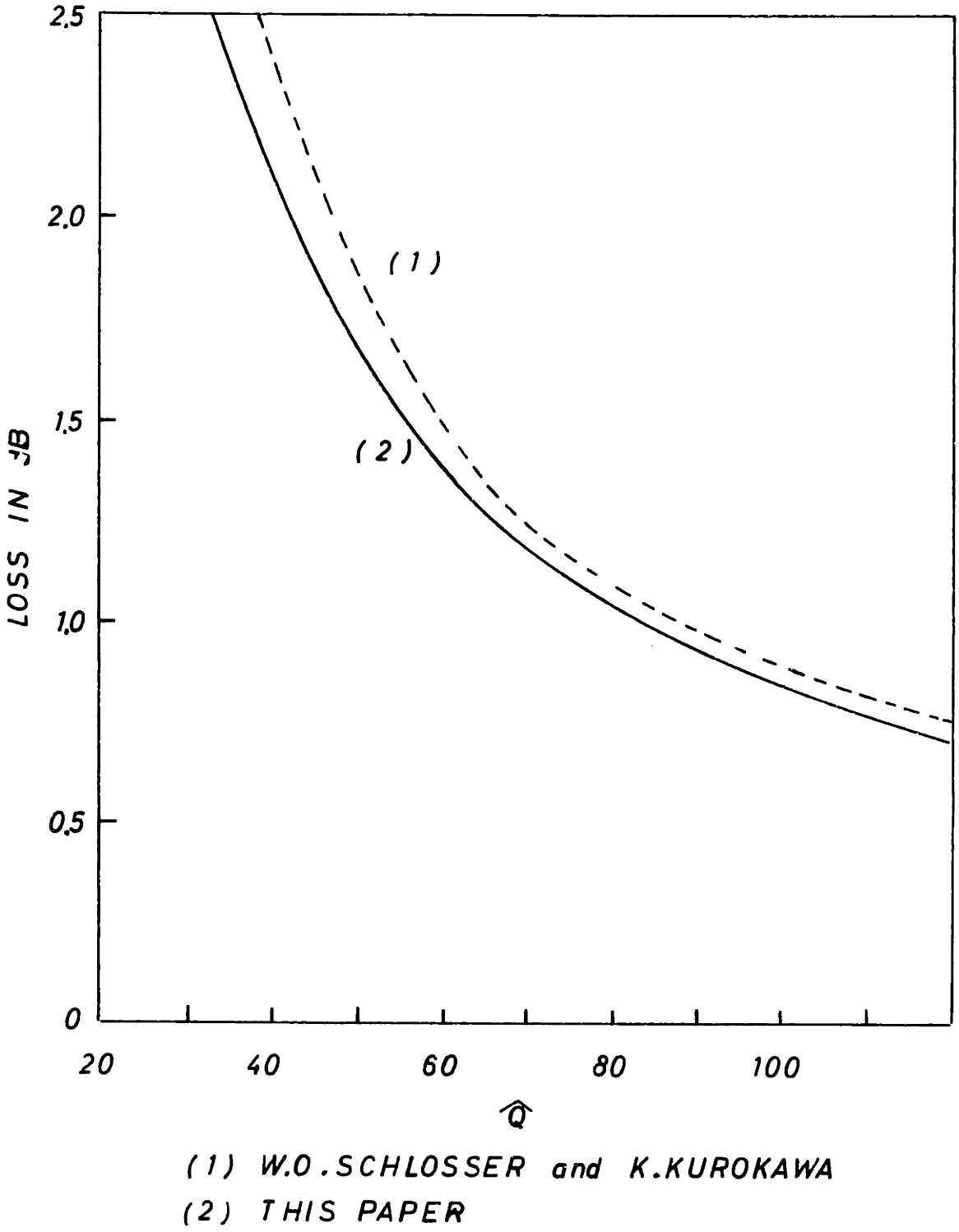

Fig. 12. Minimum loss of a four state reflection-type modulator.

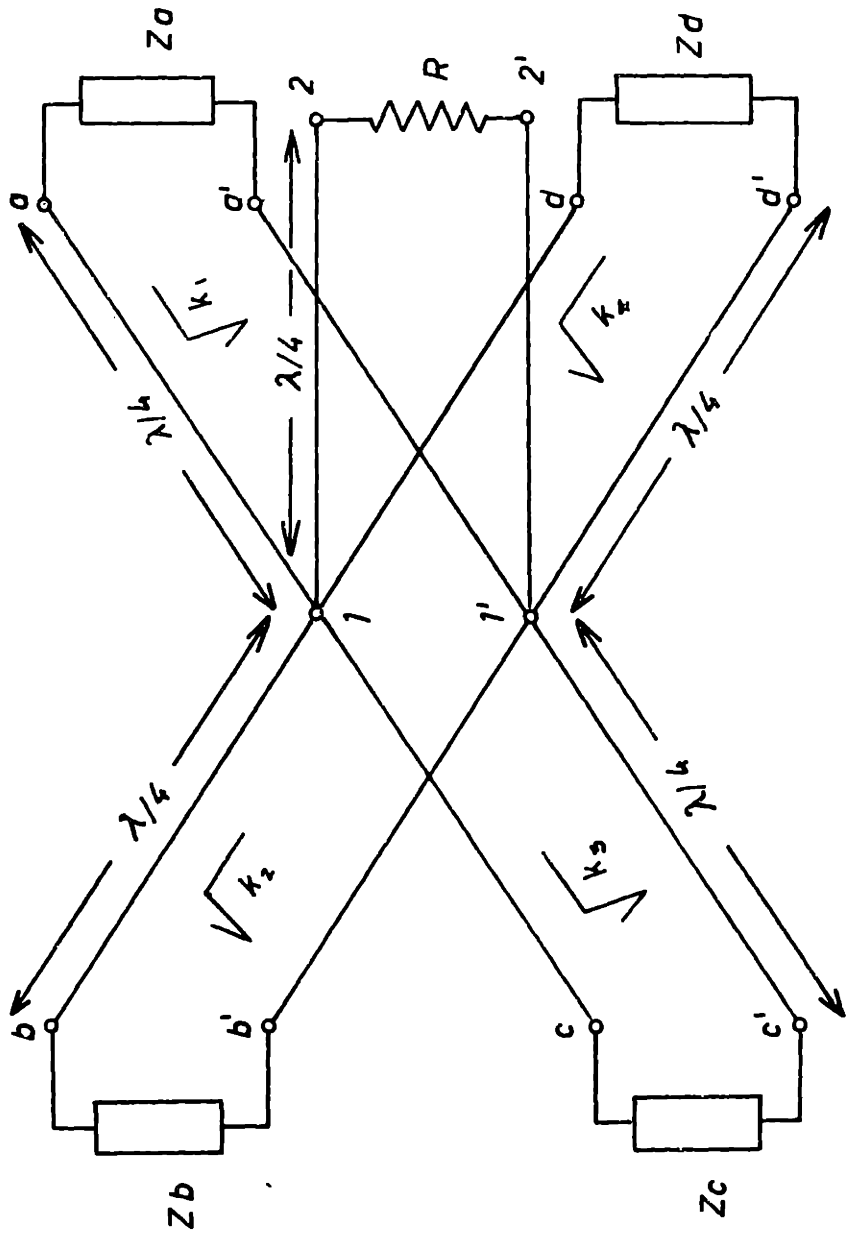

Fig. 13. An eight-state modulator.

$\frac{m_1 + m_2}{2}$	$\frac{m_2 - m_1}{2}$	$-\theta_2$
$\frac{m_1 + m_2}{2}$	$\frac{m_1 - m_2}{2}$	$-\theta_1$
$-\frac{(m_3 + m_4)}{2}$	$\frac{m_4 - m_3}{2}$	θ_4
$-\frac{(m_3 + m_4)}{2}$	$\frac{m_3 - m_4}{2}$	θ_3
$-\frac{(m_1 + m_2)}{2}$	$\frac{m_2 - m_1}{2}$	θ_2
$-\frac{(m_1 + m_2)}{2}$	$\frac{m_1 - m_2}{2}$	θ_1

The first and second columns have four different values, which can be plotted as is shown in Fig. 15. If we want identical modulators at each port of the modulator in Fig. 15, we can choose the values of k's to achieve this. For example, make $z_a = z_b = z_c = z_d = \pm j$. Then

$$\begin{aligned}
\frac{1}{k_1} &= \frac{m_3 + m_4 + m_1 + m_2}{4} \\
\frac{1}{k_2} &= \frac{m_3 + m_4 - m_1 - m_2}{4} \\
\frac{1}{k_3} &= \frac{m_4 + m_2 - m_1 - m_3}{4} \\
\frac{1}{k_4} &= \frac{m_4 - m_3 - m_2 + m_1}{4}
\end{aligned} \tag{70}$$

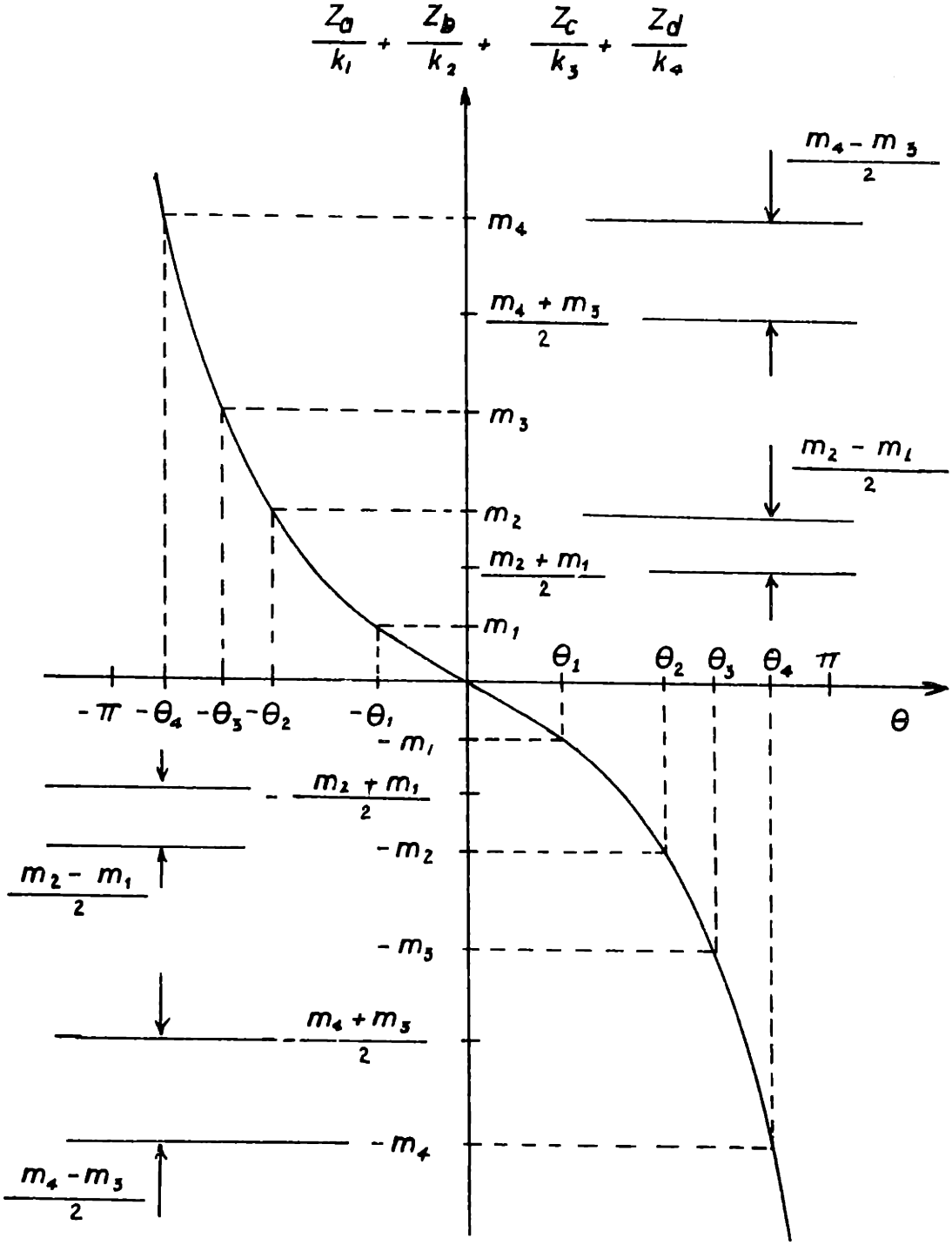

Fig. 14. Values of zin in an eight-state modulator.

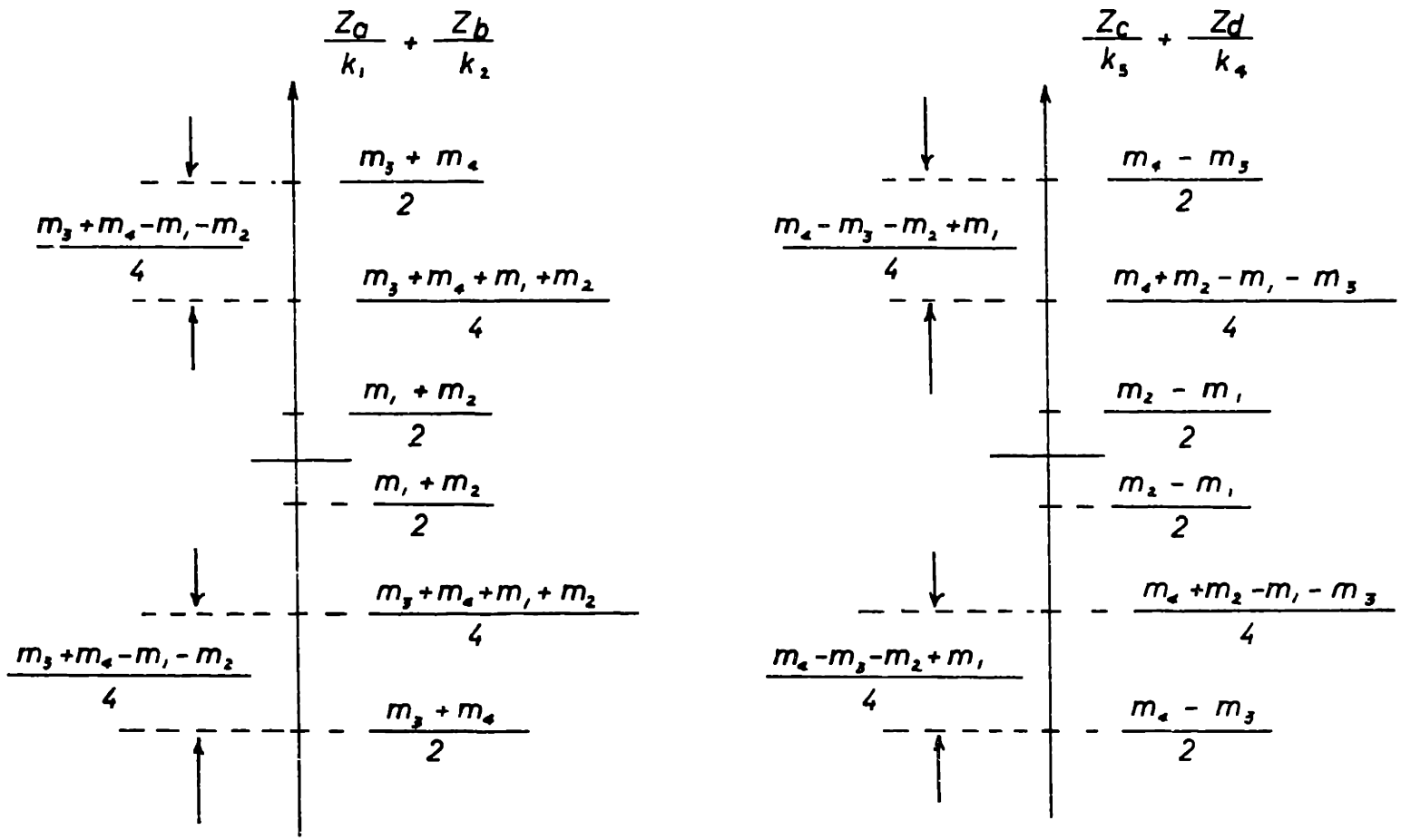

Fig. 15. Factors of zin in an eight-state modulator.

Since the states are equally spaced on the Γ-plane, for 8 states we find

$$\frac{\theta_3}{2} = \frac{\pi}{2} - \frac{\theta_2}{2}$$

$$\frac{\theta_4}{2} = \frac{\pi}{2} - \frac{\theta_1}{2} \,. \tag{71}$$

The values of (71) permit us to simplify (70). The final values are

$$k_1 = 2\left(\frac{\sin\theta_1 \sin\theta_2}{\sin\theta_2+\sin\theta_1}\right)$$

$$k_2 = 2\left(\frac{\tan\theta_1 \tan\theta_2}{\tan\theta_1+\tan\theta_2}\right)$$

$$k_3 = 2\left(\frac{\tan\theta_1 \tan\theta_2}{\tan\theta_2-\tan\theta_1}\right) \tag{72}$$

$$k_4 = 2\left(\frac{\sin\theta_1 \sin\theta_2}{\sin\theta_2-\sin\theta_1}\right).$$

Since $\theta_1 = 22.5°$ and $\theta_2 = 67.5°$, we get

$$\begin{aligned} k_1 &= 0.541197 \\ k_2 &= 0.707109 \\ k_3 &= 1 \\ k_4 &= 1.30657 \end{aligned} \tag{73}$$

6.10 LOSSES IN THE EIGHT-STATE REFLECTION-TYPE MODULATOR

As for the four-state modulator, the impedances at the ports a-a', b-b', c-c', and d-d' (Fig. 13) are the complex conjugates of themselves at the other state. Consequently, the resistive part of the input impedance will be constant, and the locus of z_{in} will be a constant resistive circle on the Smith Chart.

A parallel resistor

$$R = \frac{1}{r} = \frac{1}{\frac{r_a}{k_1} + \frac{r_b}{k_2} + \frac{r_c}{k_3} + \frac{r_d}{k_4}} \tag{74}$$

will move the 8 points to symmetric positions with respect to the center of the Smith Chart; and the losses (Fundamental Limit) will be given by

$$1 - |\Gamma|^2 = 1 - \left(\frac{1 - r}{1 + r}\right)^2. \tag{75}$$

Since $x_a = x_b = x_c = x_d = \pm j$, the resistive part of the input impedance, according to (44) and (65), will be

$$r = \frac{2}{\hat{Q}_a k_1} + \frac{2}{\hat{Q}_b k_2} + \frac{2}{\hat{Q}_c k_3} + \frac{2}{\hat{Q}_d k_4} \tag{76}$$

Any change in k_1, k_2, k_3, k_4 will not affect this value since, according to (65), the reactance will change by the

same factor [This holds under the approximations made in Appendix C]. If we assume $\hat{Q}_a = \hat{Q}_b = \hat{Q}_c = \hat{Q}_d$ and substituting (73) in (76), we have

$$r = \frac{2}{\hat{Q}} \left(\frac{1}{0.541197} + \frac{1}{0.707109} + \frac{1}{1} + \frac{1}{1.30657}\right) \tag{77}$$

Solving (77), we get

$$r = \frac{10.052}{\hat{Q}} \tag{78}$$

Equation (78) in (75) permits us to calculate the losses. A comparison between the losses in a two, four, and 8 state reflection-type modulator is seen in Fig. 16. The preceding analysis can be extended to 16 or more states. The plot of Fig. 16 shows the minimum loss in each type of modulator. However, the angle of modulation of the 2S-RM-2PI has been chosen equal to 180° in order to get the losses for equally spaced states. Therefore, in this case, the losses are the maximum.

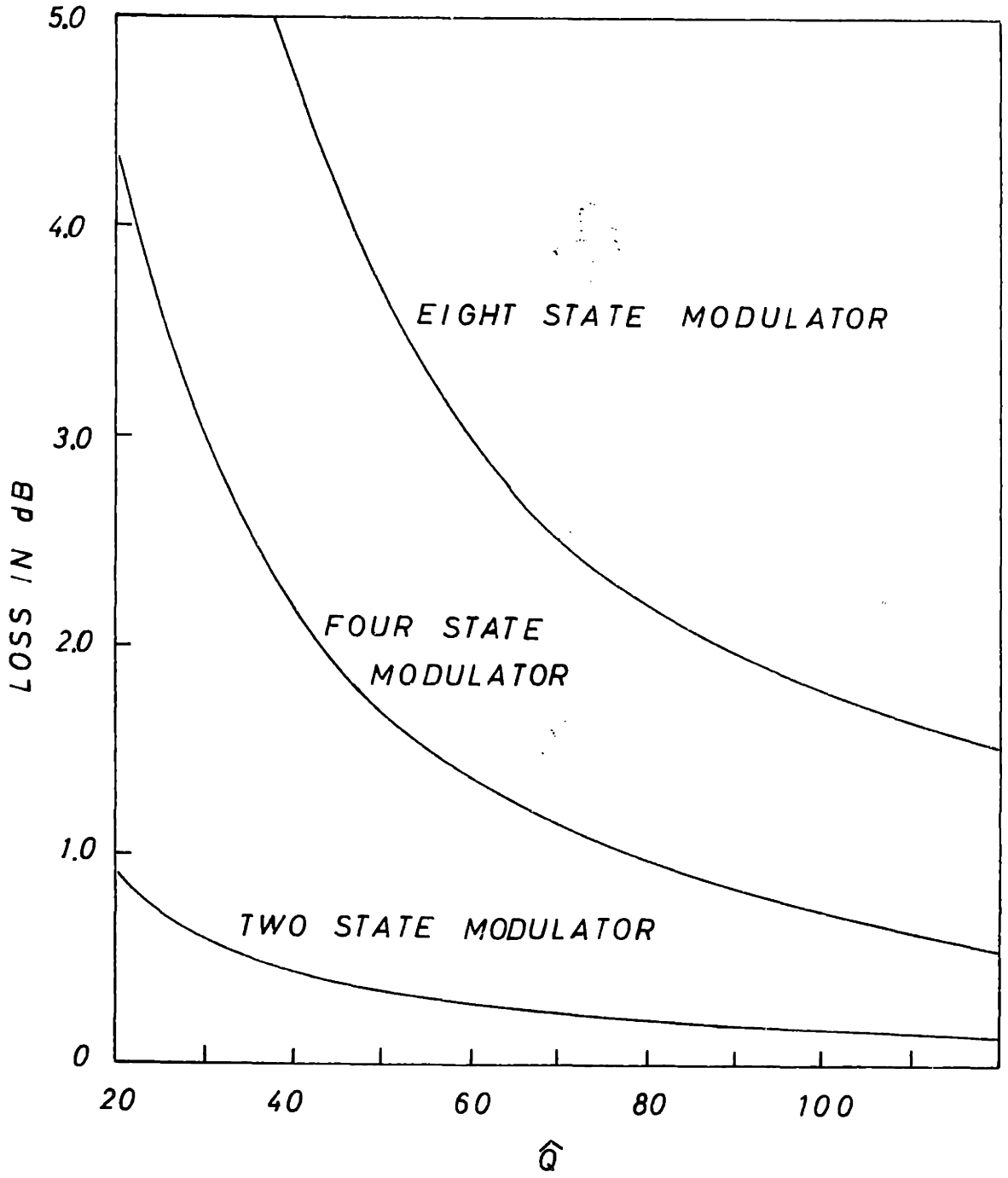

Fig. 16. Losses in an eight, four and two state reflection-type modulator for equally spaced states.

VII. TRANSMISSION-TYPE PHASE MODULATORS

DEFINITION. A transmission-type phase modulator is characterized by the scattering matrix

$$S = \begin{pmatrix} 0 & s_n \\ s_n & 0 \end{pmatrix}, \tag{79}$$

where s_n in general is a complex number quantized in n states.

DEFINITION. A network that performs (79) is identified by NS-TM-MPI, which stands for an n-state transmission-type modulator m-port imbedded.

To study transmission-type modulators and possible realizations, we shall follow a similar procedure to that for the reflection-type modulators. In this type of modulator the 2S-RM-2PI is the basic circuit unit to build up an n-state modulator.

7.1 2S-TM-3PI NETWORK

From (79), we know that input and output ports must remain perfectly matched at all times.

A well-known theorem[15] of 3-port lossless-reciprocal networks states that if two ports are simultaneously matched, the third must be decoupled. This is generally done by means of a metal post conveniently located in the

third arm of a Y- or a T-junction in waveguide inplementation. A metal post can be represented by a susceptance or a stub if we think in terms of a TEM realization.

We know that a diode can be represented by a single-valued susceptance only for a modulation angle of 0°. This means that, according to our definition of a transmission-type modulator, the 2S-TM-3PI network is a nonrealizable configuration because the two ports are simultaneously matched only for 0° of modulation on the 2S-RM-2PI network located in the third arm. If this is done, the whole system has invariant parameters with time, and no possible quantized states can exist.

7.2 2S-TM-4PI NETWORK

To get a two-state transmission modulator, we are forced to increase the number of diodes by one, and consequently the number of ports by the same amount. The most popular four-port lossless-reciprocal networks are the quadrature hybrid and the ring hybrid.

For the first one, the condition of simultaneous matching[15] at ports three and four (Fig. 17) is

$$\Gamma_1 = \Gamma_2, \tag{80}$$

where Γ_1 and Γ_2 are the reflection coefficients at ports

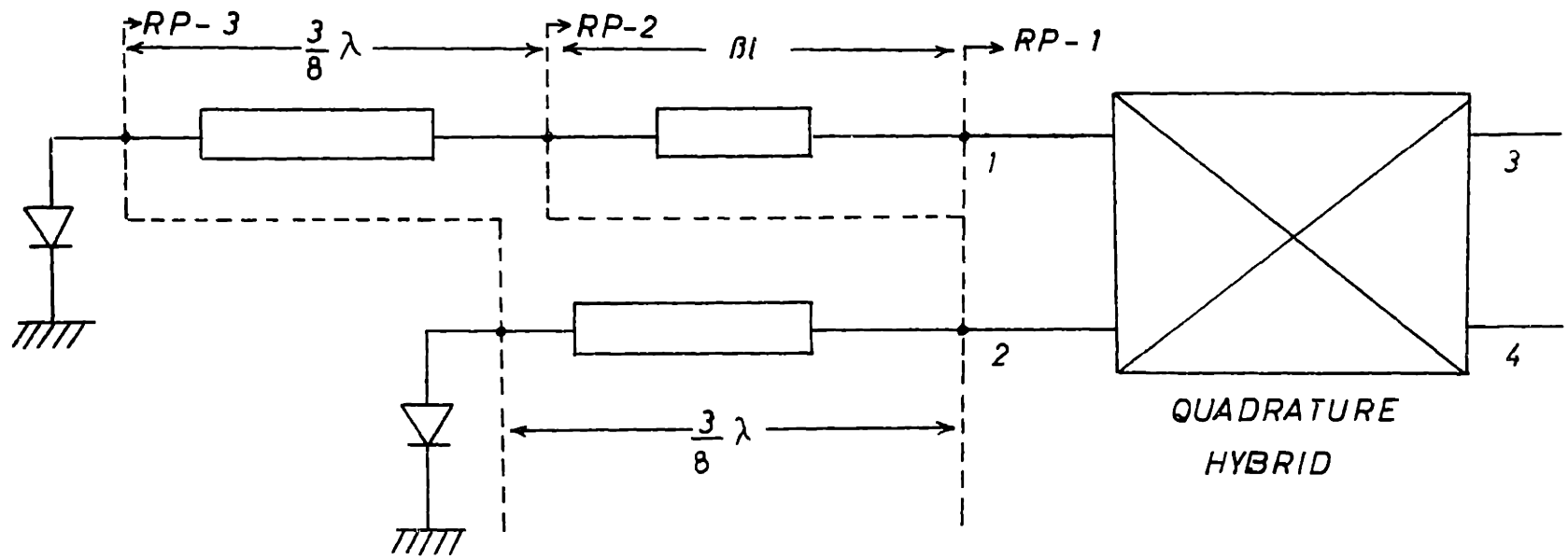

Fig. 17. Two-state transmission type modulator.

1 and 2, respectively. It is possible to get (80) by employing two 2S-RM-2PI networks with diodes perfectly matched. If the diodes are not perfectly matched, but both have the same $\hat{Q}$, then (80) is achieved by a proper extension of the length of one arm (Fig. 17). $\beta\ell$ coefficients at RP-2.

The ring hybrid is designed in a similar way, but a $\lambda/4$ piece of line should be added to one arm, in order to get

$$\Gamma_1 = -\Gamma_2 \tag{81}$$

which is a necessary condition[16] for simultaneous match at ports 3 and 4.

To emphasize the importance of a perfect match between diodes, we write the expression of the absorbed power at the input of a 2S-TM-4PI network. In the case of a quadrature hybrid we have[16]

$$P_3 = \frac{1}{2}\left(|a_3|^2 - \left|\frac{\Gamma_1 + \Gamma_2}{2} a_3\right|^2\right), \tag{82}$$

where a_3 is the input signal, and Γ_1 and Γ_2 are the reflection coefficients at ports 1 and 2, respectively.

If a phase shift exists between Γ_1 and Γ_2, these reflection coefficients can be expressed (see Appendix a) as

$$\Gamma_1 = \frac{\hat{Q}_{\phi_1}}{\sqrt{\hat{Q}^2_{\phi_1} + 4}}$$

$$\Gamma_2 = \frac{\hat{Q}_{\phi_2}}{\sqrt{\hat{Q}^2_{2} + 4}} e^{j\theta}. \tag{83}$$

Substituting (83) in (82) gives

$$P_3 = \frac{1}{2}\left[1 - \left|\frac{\hat{Q}^2_{\phi_1}}{4(\hat{Q}^2_{\phi_1} + 4)} + \frac{\hat{Q}^2_{\phi_2}}{4(\hat{Q}^2_{\phi_2} + 4)} - \frac{\hat{Q}_{\phi_1}\hat{Q}_{\phi_2} 2\cos\theta}{2\sqrt{(\hat{Q}^2_{\phi_1} + 4)(\hat{Q}^2_{\phi_2} + 4)}}\right|\right]|a_3|^2. \tag{84}$$

7.3 LOSSES IN A 2S-TM-4PI NETWORK

When the modulator is properly designed the losses are given by

$$1 - |\Gamma_n|^2 = \frac{4}{\left|\frac{\hat{Q}^2}{2(1 - \cos\phi)} + 1\right|^{1/2} + 1} \tag{85}$$

7.4 4S-TM-4PI NETWORK

Since the constraint of simultaneous matching and the input and output ports of a quadrature hybrid determine that symmetric configurations at the other ports must be

used, a 4-state transmission-type modulator is designed by employing a 4S-RM-3PI network at ports 1 and 2 of a quadrature hybrid (Fig. 18).

Condition (81) is satisfied only if the 4S-RM-3PI networks are identical. The asymmetric junction permits a straightforward design of the 2S-RM-2PI network. The 4S-TM-4PI network has two remarkable advantages compared with the standard 4-state modulator shown in Fig. 19.

1. It reduces the number of hybrids by a factor of two. This fact not only has economic advantages and simplifies the circuit, but what is more important, it reduces the losses considerably if the implementation is made in microstrip.
2. It has two diodes connected at ports 1 and 2 (Fig. 17) instead of one diode, hence the power-handling capacility is increased by a factor of two. This makes it possible to increase the output power by using the same diodes as in the circuit of Fig. 19.

7.5 CASCADING FOUR-STATE TRANSMISSION-TYPE MODULATORS

It is possible to get $2^{n/2}$ states, where n is the number of diodes, by cascading 4S-TM-4PI networks.

To illustrate the design procedure, we shall design

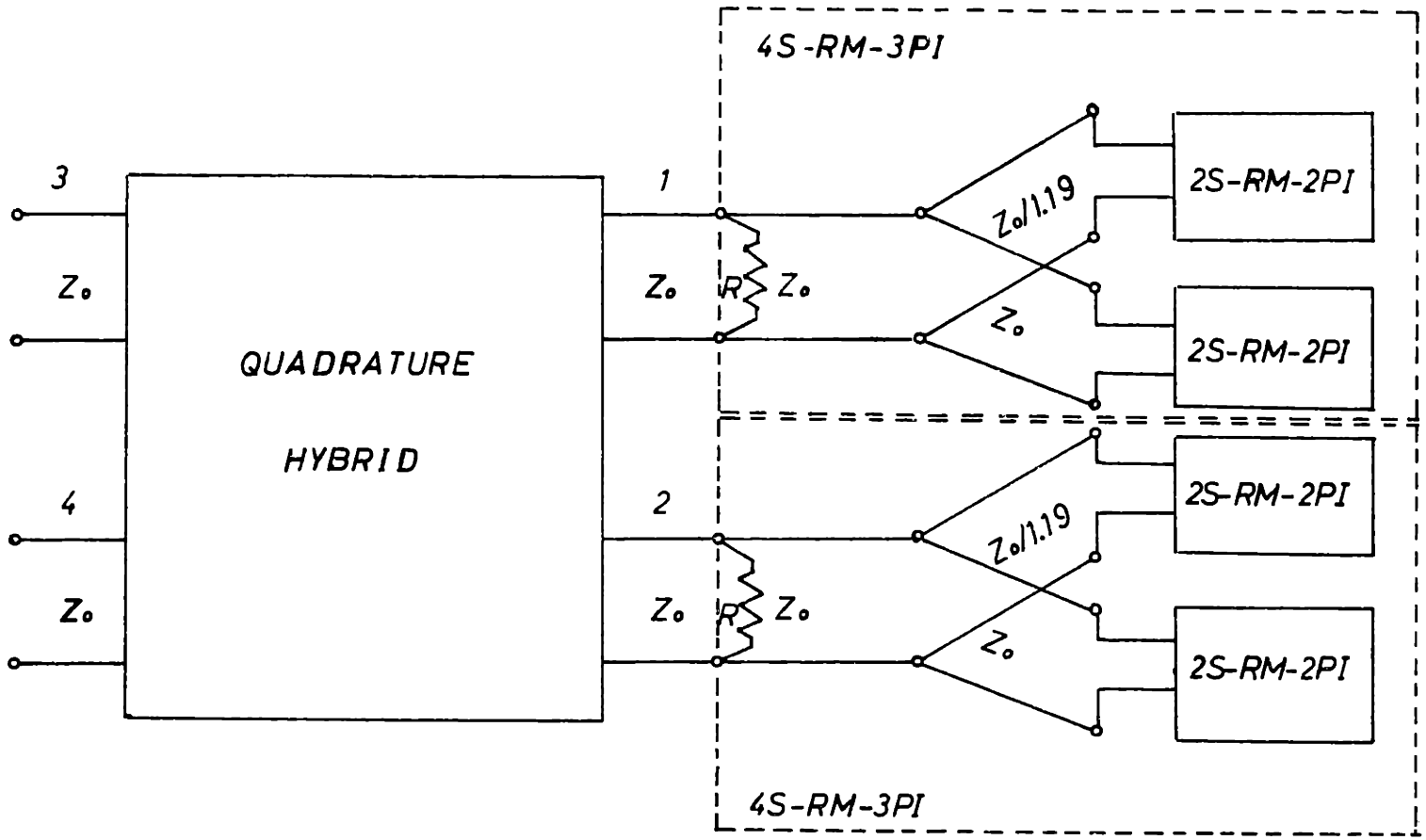

Fig. 18. Four state transmission type modulator.

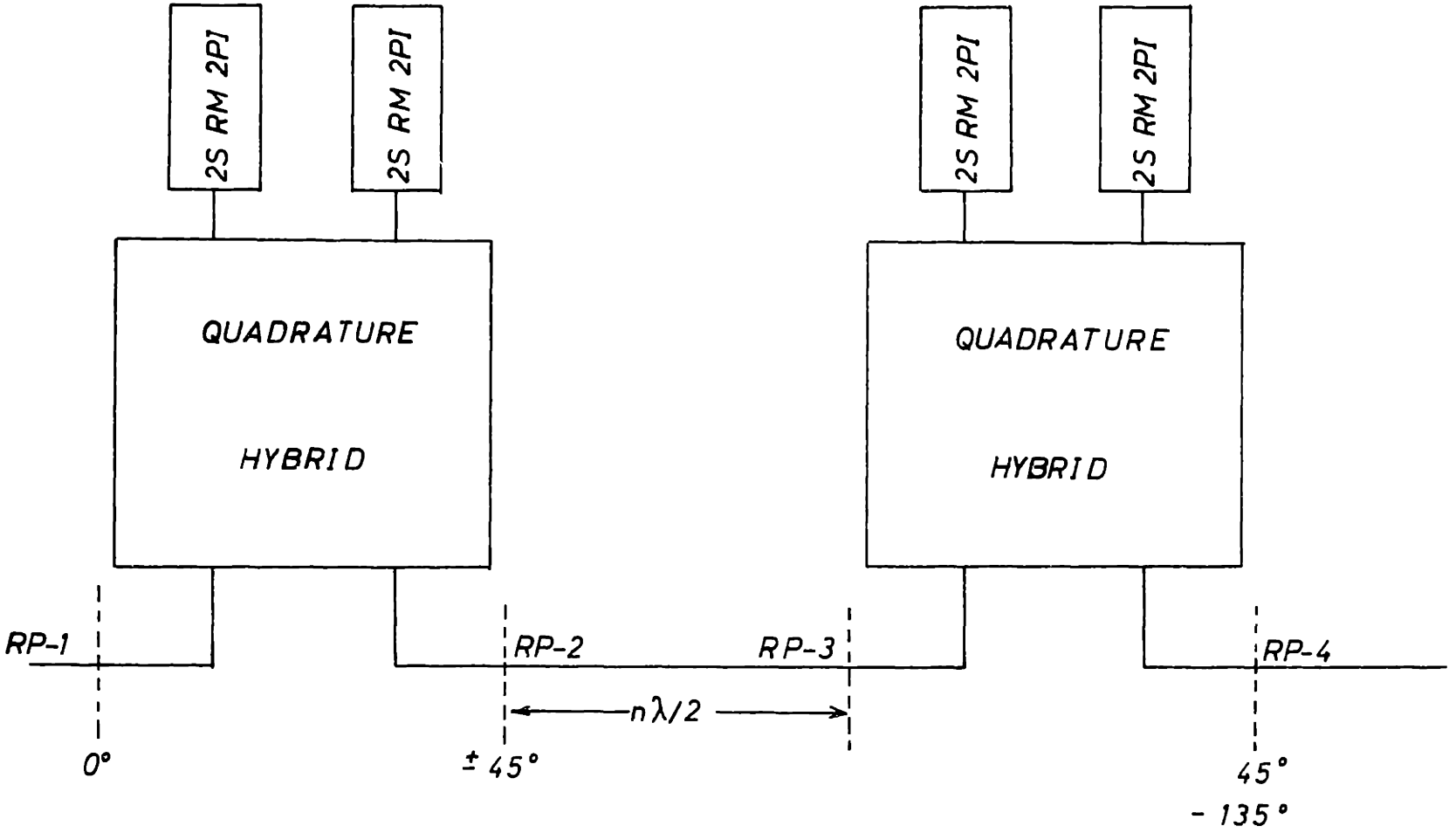

Fig. 19. Cascaded four state modulator.

a 16S-TM-6PI network. Suppose that in the circuit of Fig. 20 we have a 4S-TM-4PI network at the hybrid of the left hand. Also suppose that the four states are equally spaced, with the angles indicated at RP-2. If we draw these points on the Smith Chart, we see that the second 4S-TM-4PI network should be designed for the angles indicated at RP-4. A combination of angles at RP-2 and RP-4 will give 16 equally spaced states. If we want 64 states, another 4S-TM-4PI network is needed with angles equal to the preceding section divided by 4.

Now a question arises: How should a 4S-TM-4PI network be designed with states equally spaced but shrunk toward the 0° phase value? To answer this question, remember that first we need a 4S-RM-3PI network of the same characteristics as the transmission modulator. When we discussed the 4S-RM-3PI network, we found it useful to employ asymmetrical junctions, to get identical conditions at ports a-a' and b-b' (Fig. 10).

We shall repeat the analysis and solve (49) for the values of indicated at RP-4 (Fig. 20).

The four combinations are

$$\frac{z_{a_1}}{k} + z_{b_1} = j0.30335$$

$$\frac{z_{a_2}}{k} + z_{b_1} = -j0.0985 \qquad (86)$$

$$\frac{z_{a_1}}{k} + z_{b_2} = +j0.0985$$

$$\frac{z_{a_2}}{k} + z_{b_2} = -j0.3035.$$

From (86), we find

$$\frac{z_{a_1}}{k} = j0.200925$$

$$\frac{z_{a_2}}{k} = -j0.200925 \qquad (87)$$

$$z_{b_1} = j0.102425$$

$$z_{b_2} = -j0.102425.$$

If we make k = 0.506 in (86), we shall get identical conditions for the design of the 2S-RM-2PI modulators. In this case

$$z_a = z_b = \pm j0.102425. \qquad (88)$$

The modulation angles of the 2S-RM-3PI modulator will be

$$\frac{\phi_a}{2} = \frac{\phi_b}{2} = 2 \tan^{-1} 0.102425$$

and the full angle of modulation will be

$$\phi_a = \phi_b = 23°50'. \tag{89}$$

Four 2S-RM-2PI networks for angles of modulation given by (89) with dissimilar or identical diodes can perform the 4S-RM-3PI network to get a 4S-TM-4PI network with modulation angles of ± 11.25° and ± 33.75°, as is indicated at RP-4 (Fig. 20).

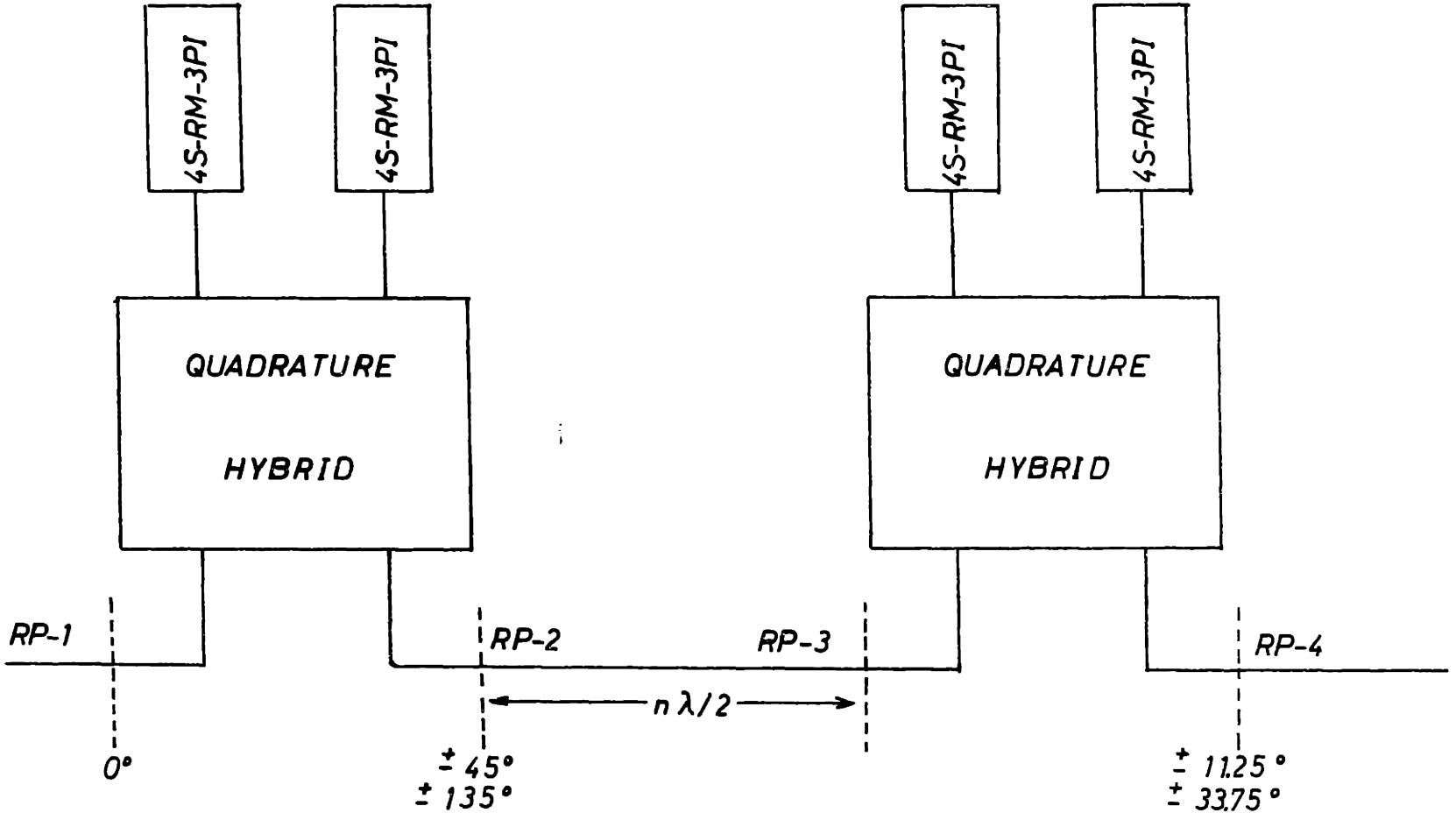

Fig. 20. Cascade 16 -state transmission-type modulator.

VIII. CONCLUSION--MEASUREMENTS AND RESULTS

Several modulator have been built, and the results are in agreement with theory.

Reflection-type phase modulators for modulation angles of 45°, 90°, and 180° were designed. We found that the 180° phase modulator is the most difficult to implement. According to Fig. 4, the $\hat{Q}_\phi$ is almost the same for angles greater than 135°, which makes the matching condition very sensitive to tolerances in the network.

For lower values (90°-45°) great accuracy can be obtained with tolerances of ± 1. This must be considered in the design of reflection or transmission-type modulators of more than two states.

We have shown that with proper choice of the characteristic impedances of the transmission line, the ON-OFF characteristic of the diodes can be adjusted to some specified value. Since accuracy is needed, the author recommends the use of a 2S-RM-2PI network for lower angles of modulation such as the circuit unit to build up an n-state modulator.

The broadbanding technique has been tried with results predicted by theory. A frequency band equivalent to 10% of midband frequency is obtained with satisfactory results. A 2S-RM-2PI network for 90°, with a Tchebycheff matching

network[17] of 3 sections is shown in Fig. 21-A. The angle of modulation vs frequency is plotted in Fig. 22. The circuit of Fig. 21-B is a 180° 2S-RM-2PI network and the circuit of Fig. 21-C is a 180° 2S-TM-4PI network.

8.1 DESIGN EXAMPLES

(a) 2S-RM-2PI network

Diode impedances $z_1 = 0.05 + j0.9$

Normalized to 50 Ω $z_2 = .055 - j0.65$

Modulation angle $\phi = 180°$.

From Eqs. 13, 15, 16, and A9b, we get

$$\hat{Q} = 29.5525$$

$$\hat{Q}_\phi = 5.25596$$

$$z_\phi = 0.7078 + j0.0959.$$

A fixed-length matching network[12] to match this impedance to the 50 Ω line is a line of λ/8 characteristic impedance $z_a = 50|z_\phi| = 39.1665$ Ω, and a λ/4 line of characteristic impedance equal to

$$z_b = 50 \sqrt{\frac{r_\phi}{(1 - \frac{x_\phi}{|z_\phi|})}} = 49.1482 \ \Omega.$$

ϕ 90°

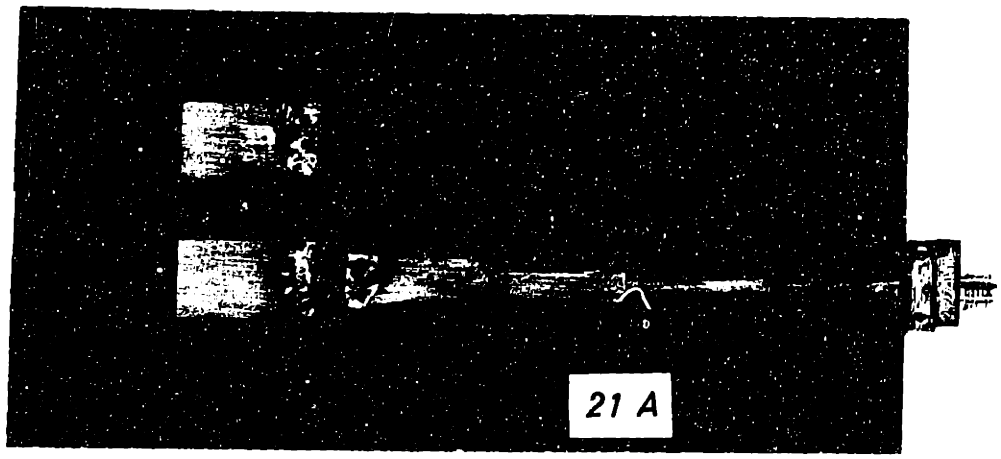

ϕ=180°

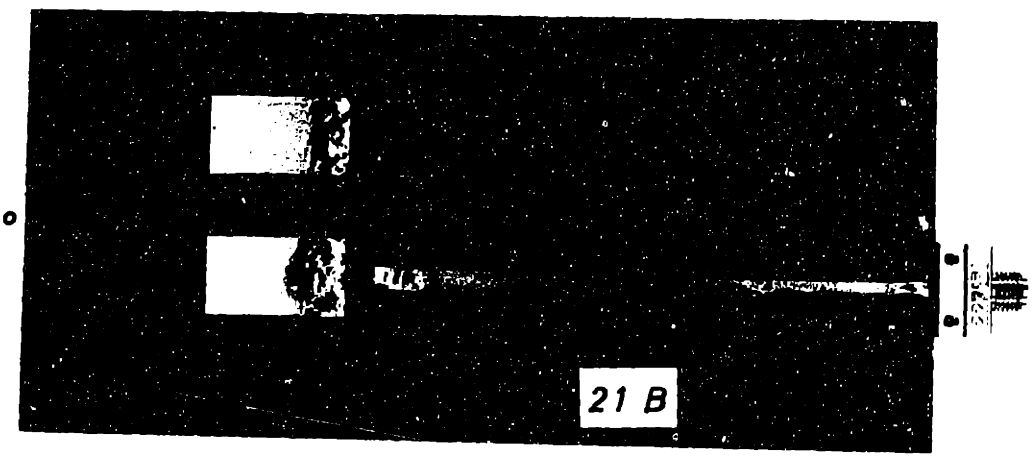

ϕ=180°

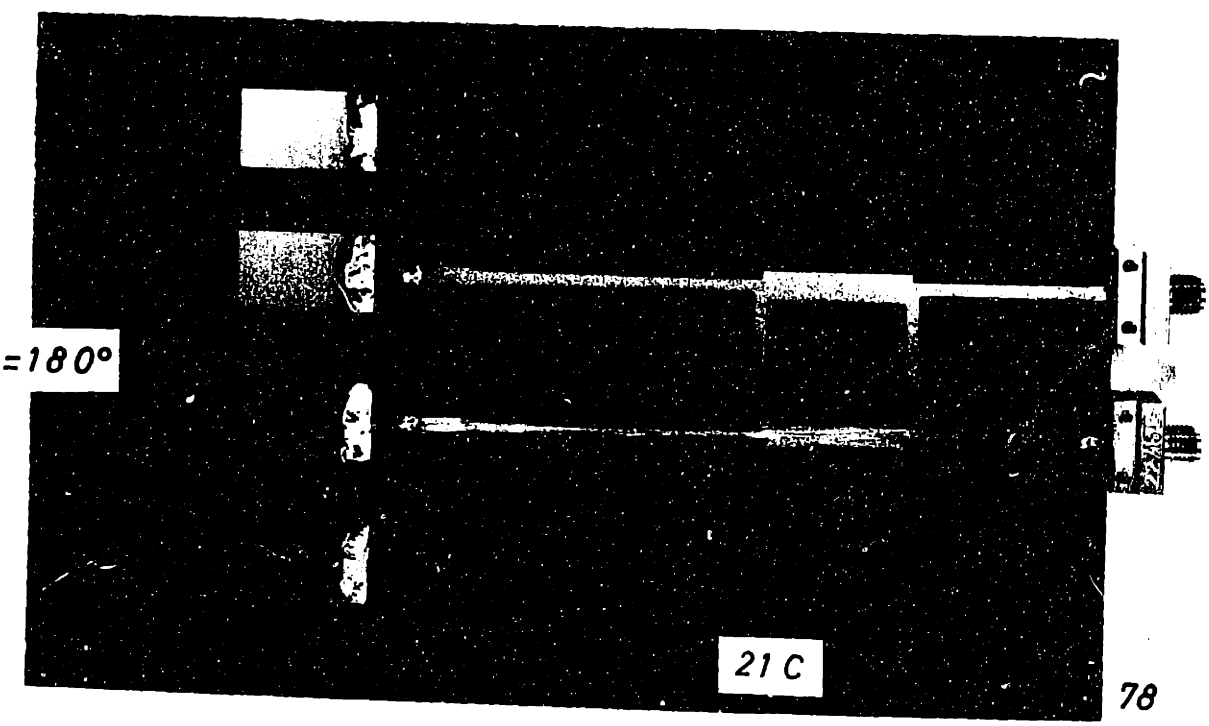

ϕ 90°

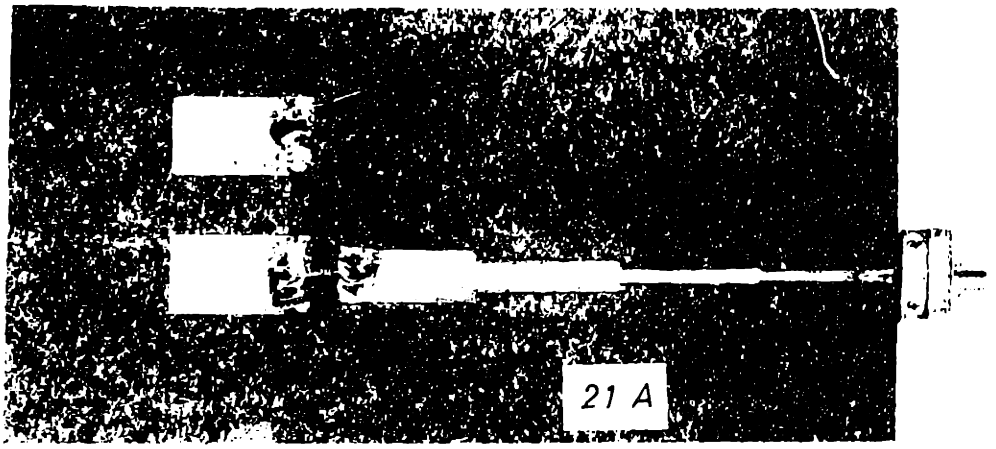

ϕ=180°

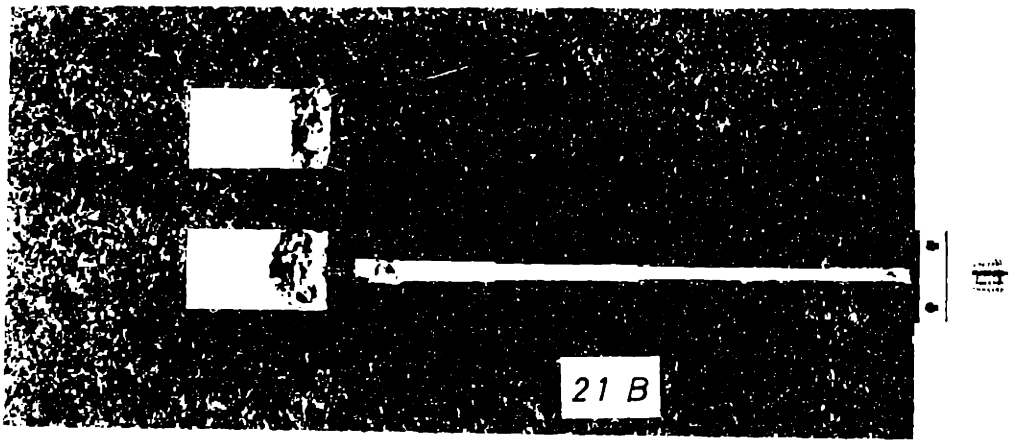

ϕ=180°

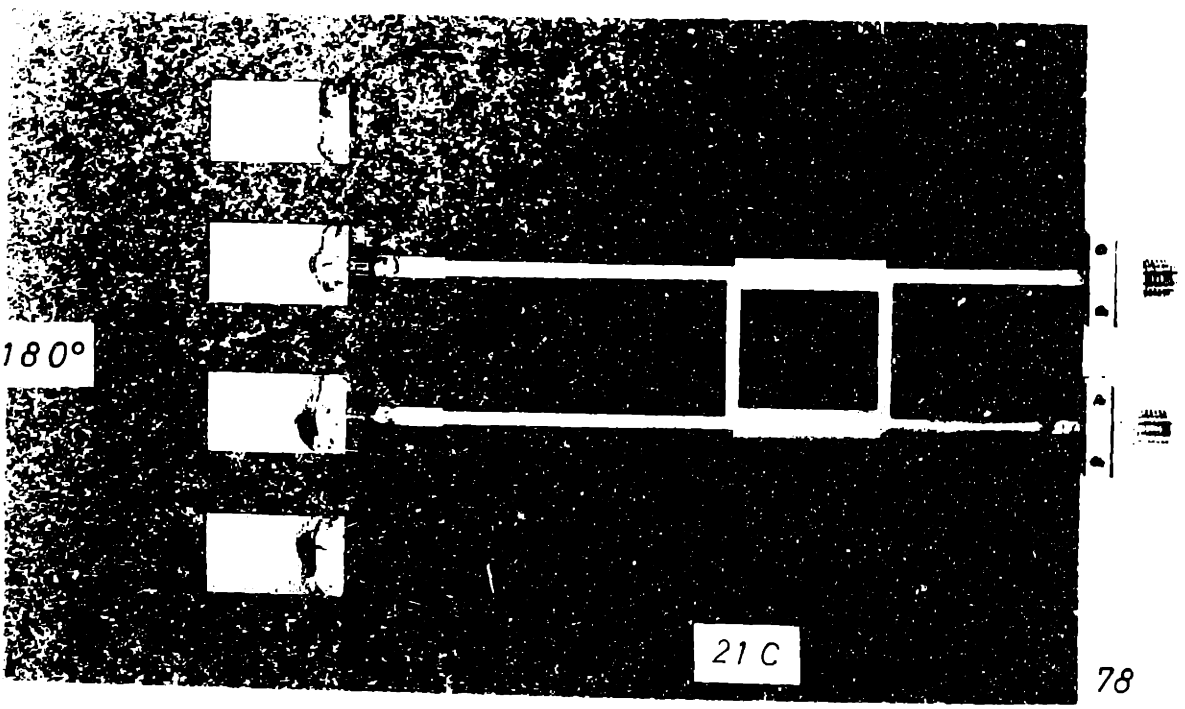

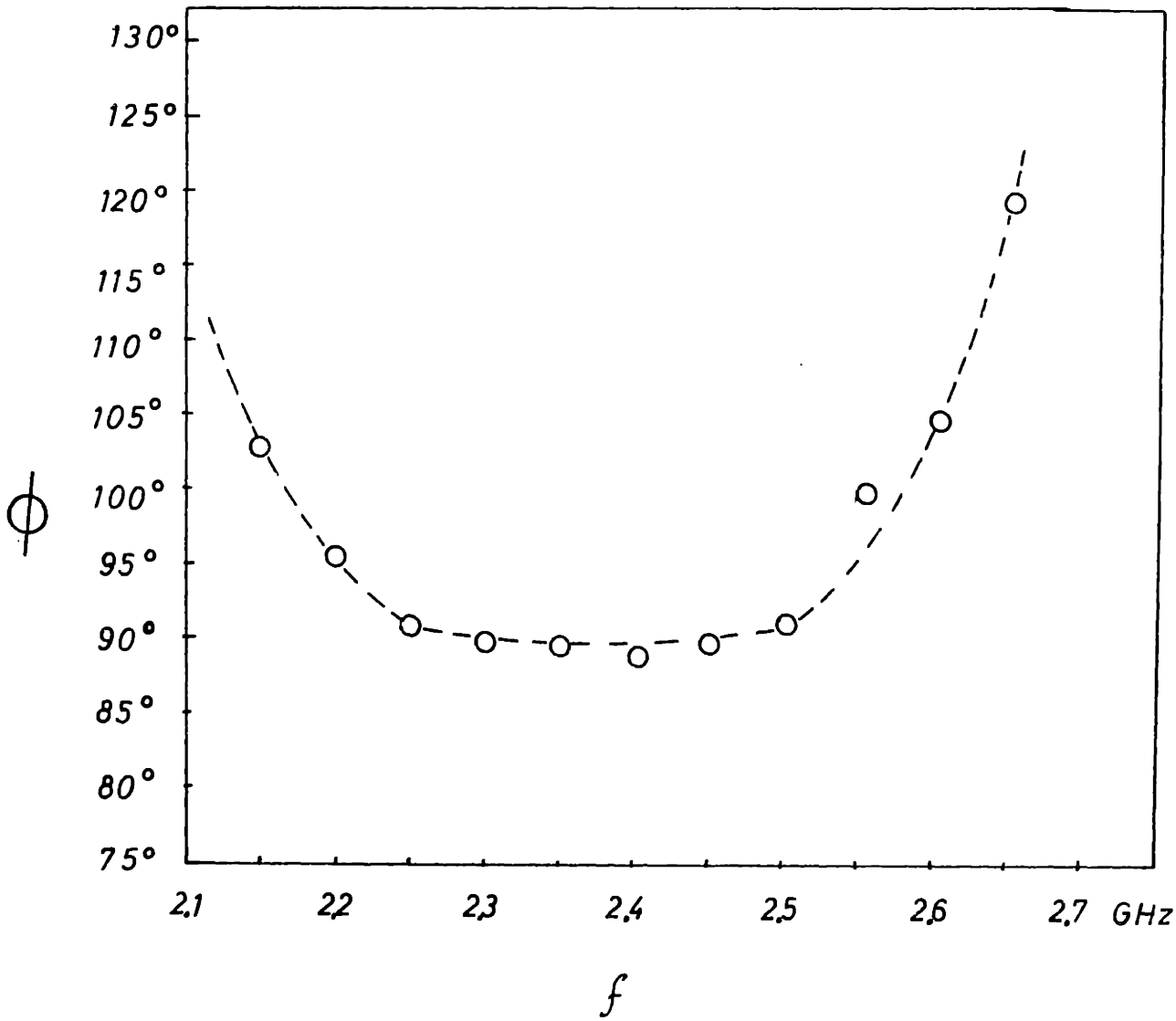

Fig. 22. Modulation angle vs frequency of a 90^{0} reflection-type modulator with broadband matching network.

When $x_\phi \to 0$, the diode is suitable for broadband operation, and the design is carried out by matching two resistive impedances.

(b) Two-state transmission-type modulator - 4PI

(i) Design of 2S-RM-3PI network

$$\text{Diode 1} = z_1 = 0.05 + j0.9$$
$$z_2 = .055 - j0.65$$

$$\text{Diode 2} = z_1 = 0.05 + j0.84$$
$$z_2 = .045 - j0.575$$

$$\phi = 180°.$$

Therefore

$$\hat{Q}_1 = 29.5575$$
$$\hat{Q}_2 = 29.831$$
$$\hat{Q}_{\phi_1} = 5.25595$$
$$\hat{Q}_{\phi_2} = 5.28189$$

$$z_{\phi_1} = 0.776396 + j0.161929$$

$$z_{\phi_2} = 0.707869 + j0.0952759.$$

Using the same matching network, we have

$$z_{a_1} = z_{\phi_{1\lambda/8}} = 39.1665\ \Omega$$

$$z_{b_1} = z_{\phi_{1\lambda/4}} = 49.1482\ \Omega$$

and

$$z_{a_2} = z_{\phi_{2\lambda/8}} = 35.669\ \Omega$$

$$z_{b_2} = z_{\phi_{2\lambda/4}} = 45.163\ \Omega.$$

(ii) Length correction in one arm

To get $\Gamma_1 = \Gamma_2$ (Fig. 17), we need to include a piece of line to correct the phase of the reflection coefficient in one arm. The reflection coefficient at RP-2, upper branch, is

$$\Gamma_1 = \frac{Z_{a_1}(z_{b_1}^2 - 50 z_1) + j(z_1 z_{b_1}^2 + z_{a_1}^2 50)}{z_{a_1}(z_{b_1}^2 + 50 z_1) + j(z_1 z_{b_1}^2 - z_{a_1}^2 50)}$$

Since $z_1 = r_1 + jx_1$, the device impedance in one state, the angle of the reflection coefficient is given by

$$\theta_1 = \tan^{-1} \frac{r_1 z_{b_1}^2 + z_{a_1}^2 50 - 50 z_{a_1} x_1}{z_{a_1} z_{b_1}^2 - 50 z_{a_1} r_1 - x_1 z_{b_1}^2} - \tan^{-1} \frac{r_1 z_{b_1}^2 - 50 z_{a_1}^2 + 50 z_{a_1} x_1}{z_{a_1} z_{b_1}^2 + 50 z_{a_1} r_1 - x_1 z_{b_1}^2}$$

For the lower branch, a similar expression is obtained with the parameters of the second matching network. Therefore

$$\beta \ell = 2\pi \frac{\alpha}{\lambda} = \theta_1 - \theta_2.$$

8.2 COMPARISON OF MATCHING NETWORKS FOR SEVERAL ANGLES OF MODULATION

In Table I is a comparison between matching networks for several angles of modulation. As we have shown, for $\phi = 180°$ there is only one equivalent matching impedance, and consequently only one solution for the matching network. Finally, for the sake of completeness, the case of asymmetric simultaneous mappings of two points on the Smith Chart has been included. We hope that in some application (certainly not for phase modulation), it may be useful. (See Appendix D).

ϕ	R_{ϕ_1}	X_{ϕ_1}	Z_{a_1}	Z_{b_1}
45°	6.9117	5.309	435.77	210.26
90°	4.3436	2.2234	243.979	141.239
135°	2.91297	1.4391	162.45	114.336
180°	2.04249	1.13797	116.905	99.7396
	R_{ϕ_2}	X_{ϕ_2}	Z_{a_2}	Z_{b_2}
45°	0.441679	0.8709	48.8258	101.05
90°	0.902438	0.911889	64.147	88.3211
135°	1.41458	0.991016	86.359	91.0889
180°	2.03908	1.13702	116.733	99.6863

diode

$z_1 = 0.6 + j2.6$

$z_2 = 1 - j1.3$

TABLE I

APPENDIX A

We shall discuss the hyperbolic distance and some quality factors.[5-7] The hyperbolic distance between two points on the Γ-plane can be obtained by applying a rigid displacement that moves one of the points to the center of the chart, and by taking the logarithm of the voltage standing wave ratio of the second point.[8,9] Let

$$z_1 = r_1 + jx_1$$

$$z_2 = r_2 + jx_2 \tag{A1}$$

be two arbitrary impedances normalized to 50 Ω. A rigid displacement in this geometry is equivalent to a lossless transformation that can be carried out as follows: (a) Add a reactance $-jx_1$. Then

$$z_1 = r_1$$

$$z_2 = r_2 + j(x_2 - x_1). \tag{A2}$$

(b) Normalize to r_1. Then

$$z_1 = 1 \tag{A3}$$

$$z_2 = \frac{r_2}{r_1} + j\left(\frac{x_2 - x_1}{r_1}\right).$$

With one point at the origin of the chart we calculate the hyperbolic distance according to the definition.

The reflection coefficient at z_2 is

$$|\Gamma_2| = \left| \frac{z_2 - 1}{z_2 + 1} \right| = \left| \frac{\frac{r_2}{r_1} + j\left(\frac{x_2 - x_1}{r_1}\right) - 1}{\frac{r_2}{r_1} + j\left(\frac{x_2 - x_1}{r_1}\right) + 1} \right| \tag{A4}$$

$$|\Gamma_2| = \sqrt{\Gamma_2 \Gamma_2^*} = \sqrt{\frac{(r_2 - r_1)^2 + (x_2 - x_1)^2}{(r_2 + r_1)^2 + (x_2 - x_1)^2}} \tag{A5}$$

where the star indicates complex conjugate.

The voltage standing-wave ratio at z_2 is

$$VSWR = \frac{1 + |\Gamma_2|}{1 - |\Gamma_2|} \tag{A6}$$

and the hyperbolic distance is given by

$$\delta = \log \text{VSWR}. \tag{A7}$$

From (A6) and (A7) we also have

$$|\Gamma_2| = \tanh \frac{\delta}{2} \tag{A8}$$

The hyperbolic distance is an invariant under lossless transformations and also all functions of δ that we may define.

Equation A5 has been proposed as a quality factor,[7] although its invariance has not been shown in a geometrical context.

Kurokawa's $\hat{Q}$ is given by

$$\hat{Q} = \frac{2}{\sqrt{\frac{1}{|\Gamma_2|^2} - 1}} \tag{A9a}$$

Substituting (A5) in (A9a) gives

$$\hat{Q} = \frac{\sqrt{(r_1 - r_2)^2 + (x_1 - x_2)^2}}{\sqrt{r_1 r_2}} \tag{A9b}$$

Also from (A9a)

$$|\Gamma_2| = \frac{\hat{Q}}{\sqrt{\hat{Q}^2 + 4}} \tag{A10}$$

Introducing (A10) in (A6), we get

$$VSWR = \frac{\sqrt{\hat{Q}^2 + 4} + \hat{Q}}{\sqrt{\hat{Q}^2 + 4} - \hat{Q}} \; . \tag{A11}$$

Substituting (A11) in (A7) gives

$$\delta = \log \left[\frac{\sqrt{\hat{Q}^2 + 4} + \hat{Q}}{\sqrt{\hat{Q}^2 + 4} - \hat{Q}} \right] \tag{A12}$$

or equivalently

$$\hat{Q} = 2 \sinh \frac{\delta}{2} \tag{A13}$$

Equations A12 and A13 express the relation between hyperbolic distance and $\hat{Q}$. A function of δ similar to (A13) has been proposed as a figure of merit for variable and nonreciprocal networks.[6]

APPENDIX B

For $\phi = 180°$, $b^2 - 4ac = 0$. Hence the condition for $x_\phi = 0$ is

$$b = 0. \tag{B1}$$

From (16)

$$\frac{2}{k_1}(x_1 - x_2) r_1 (\hat{Q}_\phi^2 + 2) - 2x_1 - 4\frac{K}{K_1^2}(x_1 - x_2) = 0 \tag{B2}$$

To simplify the analysis, it is convenient to make some approximations, based on standard characteristics of switching diodes

$$\begin{aligned} K &= x_1^2 - x_2^2 && \text{since } |r_1^2 - r_2^2| \ll |x_1^2 - x_2^2| \\ \hat{Q} &= \frac{x_1 - x_2}{\sqrt{r_1 r_2}} && \text{since } (x_1 - x_2)^2 \gg (r_1 - r_2)^2 \\ \hat{Q}_\phi^2 &= \hat{Q}^2 - 2 && \text{since } \frac{\hat{Q}^2}{4} \gg 1 . \end{aligned} \tag{B3}$$

Substituting (B3) in (B2) gives

$$\frac{2(x_1 - x_2) r_1}{(r_1 - r_2)} - 2x_1 - \frac{4(x_1 - x_2) r_1 r_2}{(r_1 - r_2)^2} . \tag{B4}$$

From (B4) we find

$$\frac{x_2}{r_2} = -\frac{x_1}{r_1}. \tag{B5}$$

APPENDIX C

For four points equally spaced on the Γ-plane, it is found that the relation between reactances at asymmetric states is the following

$$x_2 = \frac{1}{x_1}. \tag{C1}$$

Assuming that the transformed impedances due to the parallel resistor is[15]

$$z = r + \frac{x^2}{R} + jx. \tag{C2}$$

We can equate the amplitude of the reflection coefficients at two asymmetric points, and calculate the optimum value of R, to balance the four points. Therefore, (C2) and (C1) in the expression of the reflection coefficient gives

$$\sqrt{\frac{\left(r + \frac{1}{x_2^2 R} - 1\right)^2 + \frac{1}{x_2^2}}{\left(r + \frac{1}{x_2^2 R} + 1\right)^2 + \frac{1}{x_2^2}}} = \sqrt{\frac{\left(r + \frac{x_2^2}{R} - 1\right)^2 + x_2^2}{\left(r + \frac{x_2^2}{R} + 1\right)^2 + x_2^2}} \tag{C3}$$

Solving (C3), we obtain

$$r R^3 + (r^2 - 1) R^2 + r\left[\frac{1}{x_2^2} + x_2^2\right] R + 1 = 0 \tag{C4}$$

or equivalently

$$r R^3 + (r^2 - 1) R + r(x_1^2 + x_2^2) R + 1 = 0 \qquad \text{(C5)}$$

Since R is of high value, (C5), it is approximated by

$$r R^2 - R + r(x_1^2 + x_2^2) = 0 \qquad \text{(C6)}$$

Solving (C6), we get

$$R = \frac{1 \pm \sqrt{1 - 4r^2(x_1^2 + x_2^2)}}{2r} \qquad \text{(C7)}$$

Under the following condition

$$4r^2(x_1^2 + x_2^2) \ll 1 \qquad \text{(C8)}$$

Substituting (65) in (C8)

$$\frac{32(x_a + x_b)^2(x_a^2 + x_b^2)}{\hat{Q}^2} \ll 1$$

and assuming $\hat{Q}_1 = \hat{Q}_2$,

$$\hat{Q} \gg 4\sqrt{2}\,(x_a + x_b)(x_a^2 + x_b^2)^{1/2} \qquad \text{(C9)}$$

Equation (C7) can be written as: $R = \frac{1}{r}$. Now going back to (C3), and replacing $R = \frac{1}{r}$ we get the amplitude of the final reflection coefficient at four states

$$|\Gamma| = \sqrt{\frac{[r(1+x_2^2)-1]^2 + x_2^2}{[r(1+x_2^2)+1]^2 + x_2^2}} \qquad \text{(C10)}$$

Rearranging terms, we get

$$|\Gamma| = \sqrt{\frac{r^2(1+x_2^2) - 2r + 1}{r^2(1+x_2^2) + 2r + 1}} \qquad \text{(C11)}$$

The term $r^2(1 + x_2^2)$ can be neglected if

$$r^2(1+x_2^2) \ll 2r \qquad \text{(C12)}$$

From (65)

$$r^2 = 4\frac{x^2}{Q^2} \qquad \text{(C13)}$$

Substituting (C13) in (C12), we get the condition under which (C12) is valid

$$Q \gg (x_a + x_b)\left[1 + (x_a - x_b)^2\right] \qquad \text{(C14)}$$

Equation C14 is valid for $\hat{Q} > 20$, if x is approximately

less than $\frac{\sqrt{2}}{2}$. Assuming that condition (C11) will be

$$|\Gamma| = \sqrt{\frac{1-2r}{1+2r}} \tag{C15}$$

Equation C15 in a first order approximation is

$$|\Gamma| = \frac{1-r}{1+r} \tag{C16}$$

Equation C16 is a circle with its center at the origin of the Smith Chart. If we consider approximation (C9) and (C12), we conclude that the locus of z_{eq} is an elipse. We have assumed this approximation which gives the minimum losses that we can expect in a 4S-RM-3PI network; from (C8) and (C9), We see that the best way of achieving the minimum losses is designing a 2S-RM-2PI network of low angle of modulation, and selecting the reference planes at ports a-a' and b-b' of Figs. 9 and 10 in such a way as to get the ON-OFF impedances in the second and third quadrant of the Smith Chart.

APPENDIX D

Determination of z_ϕ, in the asymmetric case will be discussed.

$$\left| \Gamma_1' \right| = \left| \Gamma_2' \right| \tag{D1}$$

where Γ_1' and Γ_2' are the reflection coefficients corresponding to the transformed impedances z_1' and z_2'. Also as in the symmetric case we want a fixed angle ϕ between Γ_1' and Γ_2'.

To simplify the analysis, we define the problem in the following way: Having two impedances z_1 and z_2, a lossless reciprocal imbedding network is needed to transform the impedances to z_1' and z_2', respectively, in such a way that the reflection coefficient Γ_1' corresponding to z_1' satisfies

$$\left| \Gamma_1' \right| = \gamma, \tag{D2}$$

where γ is a real constant, previously specified.

The maximum value of γ according to (A8) will be

$$\gamma_{max} = \tanh \frac{C}{2} \tag{D3}$$

where C is the hyperbolic distance between z_1 and z_2 (Fig. D1). In terms of $\hat{Q}$, C is expressed as

$$C = \log \left[\frac{\sqrt{\hat{Q}^2 + 4} + \hat{Q}}{\sqrt{\hat{Q}^2 + 4} - \hat{Q}} \right] . \tag{D4}$$

The minimum value of γ is zero. Therefore,

$$0 \leq \gamma \leq \tanh \frac{C}{2} \tag{D5}$$

Since γ is given, the hyperbolic distance B (Fig. D1) according to (A8) is given by

$$B = 2 \tanh^{-1} \gamma . \tag{D6}$$

With values of two sides of the triangle z_ϕ, z_2, z_1 and one angle (ϕ), we proceed to solve a general triangle in non-Euclidean hyperbolic geometry. The following relation is useful.

$$\cosh C = \cosh A \cosh B - \sinh A \sinh B \cos \phi . \tag{D7}$$

From (D5), solving for sin hA, after some manipulation, we find

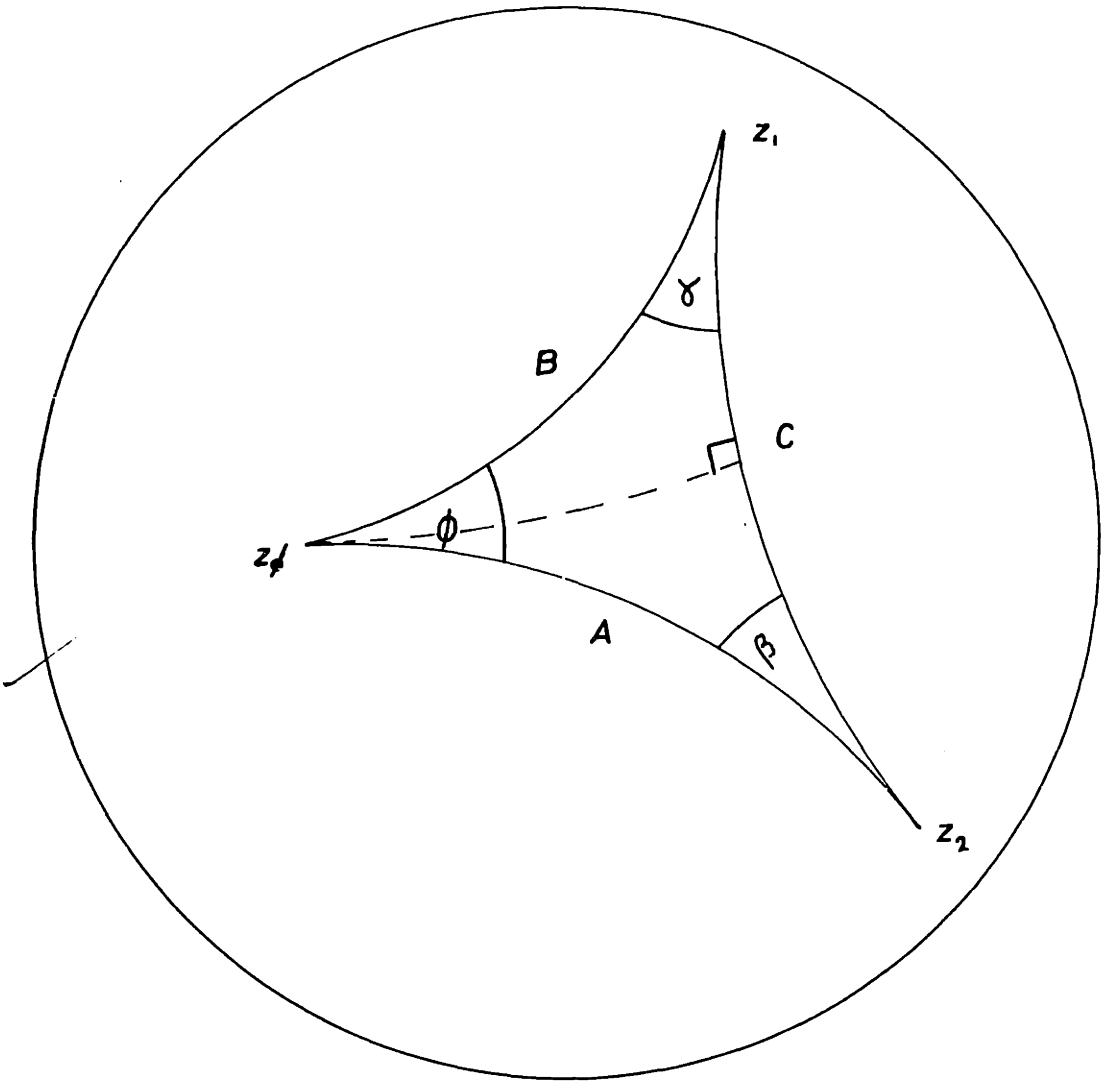

Fig. D-1. Asymmetric mapping of two impedances.

$$\sinh A = \frac{-\sinh B \cosh C \cos\phi \pm \sqrt{\cosh^2 C \cosh^2 B - \cosh^2 B \sinh^2 B \cos\phi - \cosh^4 B}}{\sinh^2 B \cos^2\phi - \cosh^2 B} \qquad \text{(D8)}$$

Hence, A is known, and the value of K is

$$K = \frac{\gamma'}{\tanh A} \cdot \qquad \text{(D9)}$$

With the values of A and B, we calculate from (A13)

$$\begin{aligned} \hat{Q}_1 &= 2\sinh\frac{A}{2} \\ \hat{Q}_2 &= 2\sinh\frac{B}{2} \end{aligned} \qquad \text{(D10)}$$

Equations D10 permit us to write two simultaneous equations as in (14), to get (15) and (16) with

$$K_1 = r_1\left(2+\hat{Q}_1^2\right) - r_2\left(2+\hat{Q}_2^2\right) \qquad \text{(D11)}$$

In the asymmetrical case, we get four solutions, since (D8) has two solutions. This fact can be understood by means of a graphical analysis.

REFERENCES

1. M. E. Hines; "Fundamental Limitations in RF Switching and Phase Shifting Using Semiconductor Diodes," Proc. IEEE 52, 697-708 (1964).

2. R. C. Mackey; "Some Characteristics of Microwave Balanced Modulators," IRE Trans. on Microwave Theory and Techniques, Vol. MTT-10, No. 2, pp. 114-117, March 1962.

3. R. V. Garver; "Theory of TEM Diode Switching," IRE Trans. on Microwave Theory and Techniques, Vol. MTT-9, pp. 224-238, May 1961.

4. J. F. White; "High Power, p-i-n Diode Controlled, Microwave Transmission Phase Shifters," IEEE Trans. on Microwave Theory and Techniques, Vol. MTT-13, pp. 233-242, March 1965.

5. K. Kurokawa and W. O. Schlosser; "Quality Factor of Switching Diodes for Digital Modulation," Proc. IEEE 58, 180-181 (1970).

6. T. Schang-Pettersen and A. Tonning; "On the Optimum Performance of Variable and Nonreciprocal Networks," IRE Trans. on Circuit Theory, Vol. CT-6, pp. 150-158, June 1959.

7. S. Kawakami; "Figure of Merit Associated with a Variable-Parameter One-Port for RF Switching and Modulation," IEEE Trans. on Circuit Theory, Vol. CT-12, pp. 321-328, September 1965.

8. G. A. Deschamps, "Geometric Viewpoints in the Representation of Waveguides and Waveguide Junctions," Proc. of the Symposium on Modern Network Synthesis, Polytechnic Institute of Brooklyn, April 16, 17 and 18, 1952, Vol. 1, pp. 277-293.

9. R. L. Khyl, "The Use of Non-Euclidean Geometry in Measurements of Periodically Loaded Transmission Lines," IRE Trans. on Microwave Theory and Techniques, Vol. MTT-14, pp. 111-115, April 1956.

10. H. Meschkowski, Non-Euclidean Geometry (Academic Press, Inc., New York).

11. M. S. Navarro, Quarterly Progress Report No. 106, Research Laboratory of Electronics, M.I.T., Cambridge, Mass., July 15, 1972, pp. 23-27.

12. D. H. Steinbrecher, "An Interesting Impedance Matching Network," IEEE Trans. on Microwave Theory and Techniques, Vol. MTT-15, No. 6, p. 382, June 1967.

13. H. A. Watson; (editor) Microwave Semiconductor Devices and Their Circuit Applications (McGraw-Hill Book Co., New York, 1969).

14. R. M. Fano, "Theoretical Limitations on the Broadband Matching of Arbitrary Impedances, Franklin Inst. 249, 57-83; 139-154 (January 1950).

15. W. O. Schlosser and K. Kurokawa, "Insertion Loss of 4-Level Phase Switch," IEEE Trans. on Microwave Theory Tech. (short papers), Vol. MTT-20, pp. 614-616, Sept. 1972.

16. J. L. Altman, Microwave Circuits (D. Van Nostrand Co., Inc., New York, 1964).

17. Matthaei, et al, Design of Microwave Filters, Impedance-Matching Networks, and Coupling Structures, Jan. 1963, Chap. 6.